Winter matters: year-round metabolism in temperate water bodies

North[1], R.L., Venkiteswaran[2], J. J., Silsbe[3], G., Harrison[4], J.W., Hudson[5], J.J., Smith[6], R.E.H,

Dillon[7], P.J., Pernica[8], P., Guildford[9], S.J., Kehoe[8,10], M., Baulch[8], H.M.

[2]Department of Geography and Environmental Studies, Wilfrid Laurier University, 75 University Avenue West, Waterloo ON N2L 3C5, Canada, ORCID 0000-0002-6574-7071
[3]Horn Point Laboratory, University of Maryland Center for Environmental Science, Cambridge, MD, United States, ORCID 0000-0003-2673-1162
[4]Hutchinson Environmental Sciences Ltd., 1-5 Chancery Lane, Bracebridge, ON, P1L 2E3, Canada, ORCID 0000-0002-6024-7166
[5]Department of Biology, University of Saskatchewan, Saskatoon, Saskatchewan, Canada, ORCID 0000-0002-0256-3240
[6]Emeritus, Department of Biology, University of Waterloo, Waterloo, Ontario, Canada
[7]Emeritus, School of the Environment and Chemistry, Trent University, Peterborough, Ontario, Canada
[8]School of Environment and Sustainability, University of Saskatchewan, Saskatoon, Saskatchewan, Canada, Baulch: ORCID 0000-0001-9018-4998, Kehoe: ORCID 0000-0002-5281-5821
[9]Emeritus, Large Lakes Observatory University of Minnesota-Duluth, Duluth, Minnesota USA, ORCID 0000-0003-0466-2872
[10]Current affiliation: Centre for Applied Research, Innovation and Entrepreneurship, Lethbridge College, Lethbridge, Alberta, Canada

Corresponding author:
[1]Rebecca North, Ph.D.
Assistant Professor of Water Quality
School of Natural Resources
University of Missouri
303L Anheuser-Busch Natural Resources Building
Columbia, MO
65211-7220
Phone: 573-882-2832
northr@missouri.edu
ORCID ID: 0000-0003-3762-5939

This paper is a non-peer reviewed preprint submitted to EarthArXiv. This manuscript has been submitted to Limnology and Oceanography for peer review. Subsequent versions of this manuscript may have slightly different content. If accepted, the final version of the manuscript will be available via the "Peer-reviewed Publication DOI" link on the right-hand side of this webpage. Please feel free to contact the corresponding author.

Twitter handle: @RebeccaNorth2

Running Head: Winter lake ecosystem metabolism

Statement of Significance

Our current understanding of lake primary productivity and metabolism is based primarily on research conducted during the open-water season. Our ability to forecast climate change impacts is hindered by our limited understanding of what happens under the ice. Our results challenge the assumption that the light climate is lower during the winter in dimictic water bodies and highlights the important role of changing light conditions on winter phytoplankton populations. This work examines the relationship between winter phytoplankton biomass and productivity with implications for year-round lake metabolism and carbon cycling. The paucity of year-round rates makes it difficult to conclude whether "most" lakes are net autotrophic or net heterotrophic. We found stochastic and brief pulses of both under-ice phytoplankton biomass and productivity that would not be captured in typical monthly monitoring programs but should be considered by all temperate aquatic ecosystem researchers.

Abstract

Winter, historically a largely un-monitored season, is important and changing. There is evidence of the importance of under-ice phytoplankton in temperate lakes, but it is currently unknown if the often high winter phytoplankton biomass translates to high productivity and what influence it has on year-round lake metabolism. Winters are getting shorter, but our ability to forecast change is hindered by our limited understanding of what happens under the ice. Here, we compare under-ice and open-water rates of areal gross production (AGP) and areal respiration (AR) from 3 Canadian reservoirs and one large lake using oxygen (O_2) changes in light-dark bottle experiments, $\delta^{18}O$-O_2 models, and fluorometry. During the open-water season, AGP was 81× greater than under-ice rates, with AR rates 8× higher than measured during winter. Open-water samples indicated autotrophy (P:R= 1.10). Consistent with current assumptions, the cold under-ice environment is associated with low primary productivity. Our results challenge the assumption that mean water column irradiance is lowest during the winter in dimictic water bodies; we find similar light conditions during the open-water season. Winter mean light is regulated by snow thickness; upon manual snow removal, we observe a 67 % increase in under-ice mean water column irradiance. The first-ever under-ice application of the $\delta^{18}O_2$-method indicated that AGP responded to improvements in light. This study reveals further insights into the importance of under-ice metabolism on year-round processes in a changing climate.

Introduction

Winter has often been thought of as a time of dormancy, or a reset button. Enhanced awareness of winter processes in lakes; however, is shifting this paradigm that assumes minimal activity under the ice in winter (Wetzel 2001); an assumption that has not been supported in recent ecological (Hampton et al. 2017; McMeans et al. 2020) and biogeochemical (Powers et al. 2017a; b; Denfeld et al. 2018) studies. Emerging research in winter limnology has a common message- winter should not be ignored (Hampton et al. 2017; Katz et al. 2015; Denfeld et al. 2018) and its importance to structuring ecosystems differs from summer, but can be similarly influential. Winter biogeochemical research is receiving increased attention (Ducharme-Riel et al. 2015; Cavaliere and Baulch 2018; Finlay et al. 2019), and changes in underwater light climate have been linked to phytoplankton dynamics (Butts and Carrick 2017; Suarez et al. 2019; Cavaliere and Baulch 2020). The impact of changing winter light climate on primary productivity, however, is still unexplored with the exception of manipulated systems (Garcia et al. 2019; Hrycik and Stockwell 2020). Baseline, year-round data is necessary to quantify what happens under the ice, and what will happen as the duration of the ice-covered period is reduced.

Climate-induced reductions in lake ice cover will result in shorter winters (Sharma et al. 2019). Predictions indicate that the percentage of ice-free winters will increase from 2 – 60 % by the end of the current century (Magnuson et al. 2000; Livingstone and Adrian 2009). Understanding winter dynamics may be important for predicting future changes in year-round lake metabolism and ecosystem function. Under-ice, the only substantive input of oxygen (O_2) is via primary production; thus, the balance between production (P) and respiration (R) is critical to preventing winterkill and maintaining aerobic biogeochemical cycles.

Paleolimnological research has shown that fossil pigments (proxies for phytoplankton) have increased in temperate lakes, coincident with earlier ice-out (Ewing et al. 2020). Under-ice phytoplankton blooms are increasingly reported; in Lake Erie, the spring bloom is most prominent during the under-ice season (Twiss et al. 2012). Under-ice blooms are also observed in a Canadian reservoir, with Chlorophyll *a* (Chl *a*) concentrations exceeding annual mean values 15 % of times measured (Cavaliere and Baulch 2020). There is also evidence that winter sets the stage for summer phytoplankton populations (Adrian et al. 1999; Katz et al. 2015; Hampton et al. 2017). A rare long-term study in a dimictic lake reported higher winter phytoplankton biomass during mild winters (Adrian et al. 1995). Following these mild winters, the maximum open water season biomass occurred one month earlier than normal and was dominated by cyanobacteria (Adrian et al. 1995, 1999). Seasonal shifts in phytoplankton biomass and composition have significant implications for food webs, fish habitat, biogeochemical cycling, and dead zones. It is important to understand if winter blooms translate to high primary productivity and what influence they have on year-round ecosystem metabolism.

The current metabolic paradigm considers lakes to be net heterotrophic (Del Giorgio and Peters 1994; Hanson et al. 2003; Idrizaj et al. 2016) and thus net ecosystem producers of carbon dioxide (CO_2) and consumers of organic matter and O_2. This understanding, however, is based on metabolic rates that are measured during the open-water season in temperate water bodies. Studies with a wider seasonal scale are raising the possibility of aquatic systems being net autotrophic (Baehr and DeGrandpre 2004; Depew et al. 2006b; Bocaniov and Smith 2009), suggesting that infrequent sampling might miss pulses of high primary production during the winter and shoulder (spring and autumn) seasons and underestimate the P:R ratio. Winter-only metabolism estimates indicate

heterotrophy (Dokulil et al. 2014; Obertegger et al. 2017; Brentrup et al. 2021), resulting in year-round P:R ratios less than one (Wassenaar 2012; Finlay et al. 2019; Brentrup et al. 2021).

Given our current understanding of lake primary productivity and metabolism in temperate lakes is largely based on research conducted during the open-water season, our ability to forecast change is hindered by our limited understanding of what happens under the ice and what will happen under a scenario of no ice cover. Here, we report absolute rates of areal gross production (AGP) and areal respiration (AR) under ice cover over the course of 2 winters in 3 Canadian reservoirs and one large lake, representing a gradient in snow cover and morphometry, and compare estimates with open-water rates. We address the following specific questions:

1) How do under-ice rates of productivity and respiration compare with open-water rates?

2) How important are under-ice processes on year-round ecosystem metabolism?

3) What are the environmental drivers of under-ice productivity and respiration?

To address these questions, we challenge the metabolic balance paradigm by considering temperate lakes and reservoirs on a year-round basis. We hypothesize that winter productivity is important, and that current open-water perspectives on lake metabolism are not representative of the entire year in temperate lakes. To add scientific rigor to our tests, we measured under-ice community metabolism by 3 different methods. These include AGP derived from fluorometric measurements, $\delta^{18}O$-O_2-derived rates of AGP and AR, as well as traditional light/dark O_2 changes. This is the first-ever application of both the $\delta^{18}O$-O_2 and fluorometric approaches to quantifying absolute under-ice primary production. In sum, we ask: what are the implications of changing winter conditions on year-round temperate lake metabolic function? Rate measurements conducted over a full year, instead of a single season, will provide a more comprehensive understanding of the effect of a changing climate on lake ecosystems.

Materials

Study site descriptions

This study was conducted on 3 mesotrophic reservoirs in southern Saskatchewan (SK; Blackstrap, Broderick, Diefenbaker) and one oligo-mesotrophic large lake in southern Ontario (ON; Lake Simcoe; Fig. 1), Canada. All 4 water bodies are dimictic and represent a gradient in size, depth, and snow cover (Table 1). Lake Simcoe is a large (surface area = 722 km^2), shallow (mean depth = 16 m, maximum depth = 42 m; North et al. 2013), windswept lake that provides a stark contrast to the smaller SK reservoirs.

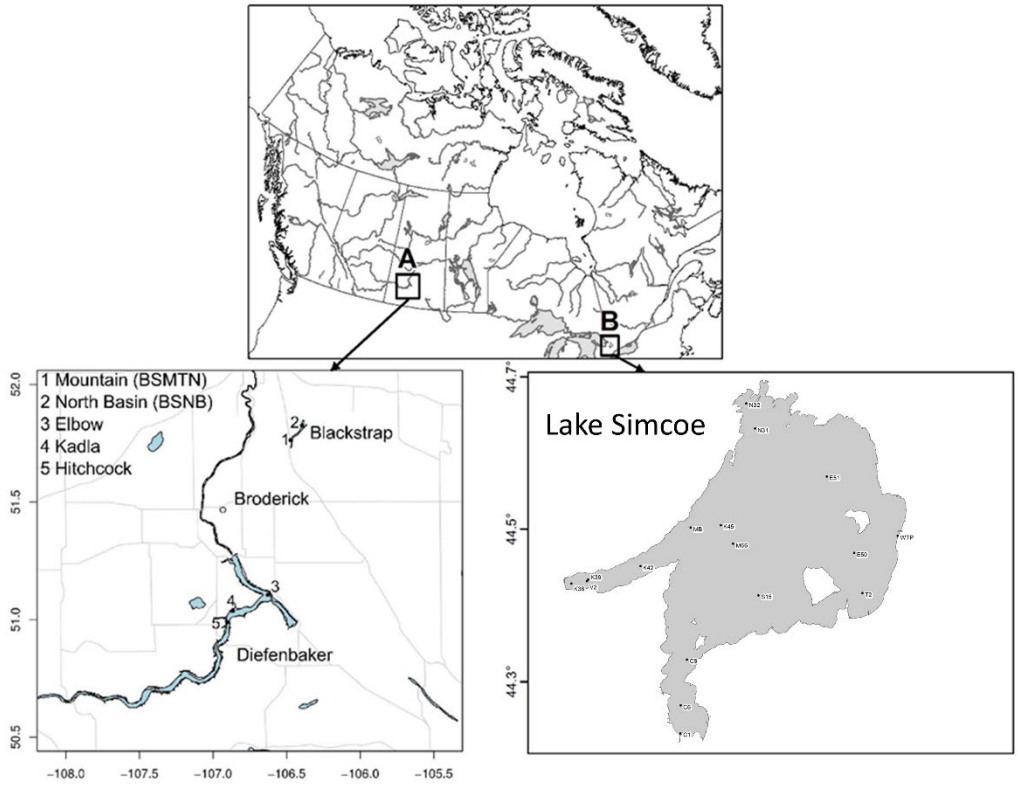

Figure 1. Map of Canadian water bodies and associated stations. A) Locations of the 3 Saskatchewan reservoirs with all sampling stations labelled: Blackstrap (1, 2), Broderick, and Diefenbaker (3, 4, 5). B) Lake Simcoe, Ontario, with all 17 stations labelled including the Beaverton water treatment plant (WTP) intake pipe.

Table 1. Physical, chemical, and biological parameters measured during the open-water and ice-covered seasons, differentiated by water body. Shown are the arithmetic mean and range (minimum, maximum) of *n* samples. Two stations were sampled on Blackstrap reservoir, one on Broderick reservoir, 3 on Diefenbaker reservoir, and 17 on Lake Simcoe (Fig. 1). NA, Not Applicable; Z, depth; PAR, Photosynthetically Active Radiation; K_d, vertical attenuation coefficient; TP, Total Phosphorus; TDP, Total Dissolved Phosphorus; DRP, Dissolved Reactive Phosphorus; TDN, Total Dissolved Nitrogen; PN, Particulate Nitrogen; NH_4^+, ammonium; NO_3^-, nitrate; Chl *a*, Chlorophyll *a*; POC, Particulate Organic Carbon; Phyto, Phytoplankton; E_k, light saturation parameter; $rETR_{max}$, maximum relative electron transport rate through PSII; α, light limited slope of the P-E curve; ANP, Areal Net Productivity; LD, light-dark bottle experiments; AGP, Areal Gross Productivity; AR, Areal Respiration; $\bar{E}_{24}$, mean daily mixed layer irradiance. S+I+W K_d values account for water (W), ice (I), and snow (S) attenuation, S+I K_d values account for ice and snow attenuation.

170

Parameter	Blackstrap Open-water (n =2)	Blackstrap Under-ice (n =9)	Broderick Open-water (n =1)	Broderick Under-ice (n =5)	Diefenbaker Open-water (n =13)	Diefenbaker Under-ice (n =9)	Simcoe Open-water (n =88)	Simcoe Under-ice (n =23)
Physical								
Z_{mix} (m)	6.8 (6.5, 7.0)	0.2 (NA, 1.0)	5.0	NA	18.0 (7.0, 37.1)	1.5 (NA, 4.5)	13.2 (2.0, 37.9)	1.1 (NA, 3.5)
Z_{snow} (cm)	NA	13.3 (0.1, 26.8)	NA	11.9 (0.7, 19.0)	NA	12.4 (1.7, 21.3)	NA	7.0 (0.1, 22.9)
Z_{ice} (cm)	NA	82.9 (58.8, 98.2)	NA	76.0 (49.3, 92.7)	NA	70.1 (57.7, 85.3)	NA	35.5 (25.4, 45.7)
$Z_{white\ ice}$ (cm)	NA	7.6 (2.7, 25.0)	NA	7.8 (5.2, 11.5)	NA	3.4 (0.0, 9.7)	NA	16.1 (10.2, 20.3)
$Z_{black\ ice}$ (cm)	NA	74.7 (54.0, 95.0)	NA	68.2 (44.1, 87.3)	NA	66.7 (56.7, 82.2)	NA	24.6 (22.9, 25.4)
Albedo	NA	1.9 (1.6, 2.3)	NA	1.8 (1.4, 2.1)	NA	1.8 (1.6, 2.1)	NA	1.1 (1.0, 1.1)

Surface PAR	1090.2	43.7	432.9	12.4	1297.3	100.2	862.8	157.8
(μmol m^{-2} s^{-1})	(966.0, 1214.3)	(3.3, 262.2)		(2.3, 37.5)	(884.9, 1760.9)	(5.7, 480.6)	(143.9, 2010.0)	(4.6, 1276.5)
Water K_d	0.8	0.6	1.0	0.4	0.7	0.6	0.3	0.3
(m^{-1})	(0.7, 0.8)	(0.4, 1.1)		(0.2, 0.7)	(0.4, 1.2)	(0.4, 0.8)	(0.2, 0.5)	(0.1, 0.5)
S+I+W K_d	NA	4.3	NA	5.1	NA	3.7	NA	NA
(m^{-1})		(0.6, 5.5)		(3.3, 7.0)				
S+I K_d	NA	3.7	NA	4.7	NA	3.0	NA	NA
(m^{-1})		(0.2, 5.0)		(2.5, 6.7)				
PAR	NA	8.7	NA	2.5	NA	20.3	NA	23.5
transmission		(1.2, 24.3)		(0.9, 5.8)		(0.7, 79.5)		(0.9, 89.6)
(%)								
$\bar{E}_{24}$	94.5	22.1	89.5	17.2	43.5	40.9	31.0	90.7
(μmol m^{-2} s^{-1})	(90.4, 98.5)	(3.7, 68.3)		(2.3, 37.5)	(19.0, 78.7)	(0.5, 223.0)	(7.4, 74.2)	(6.7, 555.6)
Chemical								
TP	1.32	1.70	0.57	0.64	0.51	0.36	0.28	0.28
(μmol L^{-1})	(1.10, 1.53)	(1.40, 1.90)		(0.53, 0.74)	(0.25, 0.89)	(0.17, 0.64)	(0.16, 0.48)	(0.22, 0.52)
TDP	0.73	1.50	0.29	0.47	0.20	0.14	0.14	0.19
(μmol L^{-1})	(0.62, 0.85)	(1.10, 1.70)		(0.28, 0.57)	(0.14, 0.57)	(0.09, 0.19)	(0.06, 0.30)	(0.11, 0.28)

DRP	0.08	0.80	0.03	0.23	0.04	0.05	0.01	0.01
(μmol L^{-1})	(0.07, 0.09)	(0.40, 1.00)		(0.07, 0.38)	(0.02, 0.09)	(0.03, 0.12)	(0.01, 0.24)	
TDN	9.1	27.5	4.3	24.3	40.6	12.0	3.5	4.0
(μmol L^{-1})	(8.2, 9.9)	(12.4, 34.2)		(10.5, 48.9)	(28.7, 60.1)	(9.8, 18.0)	(1.0, 12.9)	(0.6, 14.8)
PN	NA	1.0	NA	1.8	1.7	3.2	0.1	0.2
(μmol L^{-1})		(0.6, 1.2)		(1.0, 3.2)	(0.1, 8.8)	(1.3, 8.4)	(0.1, 0.8)	(0.1, 0.6)
NH_4^+	0.8	14.1	0.2	6.2	0.2	0.5	0.1	0.1
(μmol L^{-1})	(0.3, 1.3)	(6.4, 23.8)		(0.2, 20.5)	(0.1, 0.9)	(0.2, 0.8)	(0.1, 0.3)	(0.1, 0.2)
NO_3^-	8.3	13.4	4.2	18.1	31.0	12.1	0.2	0.2
(μmol L^{-1})	(7.9, 8.6)	(4.5, 20.5)		(10.4, 28.4)	(18.2, 41.9)	(7.3, 23.2)	(0.1, 0.7)	(0.1, 1.0)
Biological								
Chl *a*	8.4	3.1	3.8	1.4	3.3	2.1	1.7	3.2
(μg L^{-1})	(6.1, 10.6)	(0.1, 27.8)		(0.1, 2.9)	(1.0, 8.7)	(0.7, 5.6)	(0.1, 6.5)	(0.3, 13.1)
POC	NA	93.5	NA	128.3	29.9	190.1	18.1	10.7
(μmol L^{-1})		(69.1, 114.8)		(64.2, 210.1)	(9.8, 89.5)	(88.9, 412.1)	(5.2, 37.5)	(0.4, 24.5)
Phyto biomass	567.52	53.92	328.59	381.67	260.29	1372.61	NA	NA
(mg m^{-3})	(252.93, 882.12)	(35.14, 72.86)		(6.98, 1390.47)	(216.48, 317.01)	(281.90, 6407.77)		

$\bar{E}_{24}$:E_k	0.1	0.1 (0.0, 0.2)	0.3	0.1 (0.0, 0.4)	0.1 (0.0, 0.2)	0.2 (0.0, 1.3)	0.2 (0.0, 0.7)	1.4 (0.1, 10.4)
E_k (μmol m^{-2} s^{-1})	710.2	354.2 (100.0, 716.4)	333.2	308.1 (96.0, 451.1)	458.2 (340.6, 595.3)	230.3 (118.0, 464.2)	178.0 (32.1, 1000.0)	78.7 (2.7, 233.3)
$rETR_{max}$ (photons reemitted absorbed^{-1})	328.5	83.4 (0.6, 344.0)	189.9	32.9 (9.1, 58.3)	253.6 (152.8, 358.5)	53.7 (13.7, 101.3)	76.5 (13.3, 272.9)	38.2 (1.0, 62.5)
α	0.47	0.76 (0.57, 1.00)	0.57	0.60 (0.30, 0.70)	0.50 (0.40, 0.60)	0.60 (0.10, 1.00)	0.50 (0.10, 0.80)	0.70 (0.30, 4.10)
ANP- $\delta^{18}O$ (mmol O_2 m^{-2} day^{-1})	20.0 (17.9, 22.1)	-5.2 (-24.3, -1.8)	10.9	-12.9 (-33.0, -4.6)	6.5 (2.5, 9.0)	0.0 (-0.4, 0.5)	2.9 (-10.5, 19.8)	0.1 (0.0, 0.2)
ANP-LD (mmol O_2 m^{-2} day^{-1})	NA	NA	NA	NA	NA	NA	17.7 (-33.5, 107.1)	-11.9 (-55.1, 5.9)
AGP:AR-$\delta^{18}O$	1.2	0.0 (0.0, 0.3)	1.2	0.0 (0.0, 0.1)	1.1 (1.1, 1.2)	1.2 (0.6, 2.7)	1.1 (0.8, 1.7)	1.2 (1.1, 1.4)

AGP:AR-LD	NA	NA	NA	NA	NA	NA	12.6 (0.0, 55.8)	0.5 (0.0, 3.9)

171

Lake Simcoe was sampled year-round in 2010–2011 and the SK reservoirs in 2013–2014. Seventeen stations were sampled intermittently on Lake Simcoe; the most frequently sampled stations were sampled 3 times over the 6-week winter of 2011. The Lake Simcoe stations represented a gradient between nearshore (minimum station depth, 2 m) and offshore regions (maximum station depth, 42 m; Fig. 1). See North et al (2013) for a bathymetric map. On Lake Simcoe, the Beaverton water treatment plant (WTP) intake pipe was sampled from January to July, 2011 to supplement sampling during unstable ice cover (Quinn et al. 2013; Kim et al. 2015; Fig. 1). Ice-on occurred on January 6, 2011 on Lake Simcoe and November 10, 2012 and November 6, 2013 on the SK reservoirs.

Lake Diefenbaker, SK is a run-of-the-river reservoir along the South Saskatchewan River, with an area of 394 km^2, a mean depth of 22 m, and a maximum depth of 59 m. Three stations were sampled on Lake Diefenbaker representing the main channel (Hitchcock, maximum depth 25 m), an embayment (Kadla, maximum depth 11.8 m), and the deeper lacustrine region (Elbow, maximum depth 31.8 m; North et al. 2015; Fig. 1). See Sadeghian et al (2015) for a bathymetric map. Originating from the Qu'Appelle Dam on Lake Diefenbaker, gravity-fed canals transport water downstream through Broderick and Blackstrap reservoirs. Broderick reservoir has a surface area of 4 km^2, with a mean depth of 6 m and a maximum depth of 7 m; one station represents this reservoir. Blackstrap reservoir has a surface area of 12 km^2, with a mean depth of 5 m and maximum depth of 9 m. Two stations were sampled (Fig. 1), one in the north basin (Blackstrap North Basin [BSNB], depth 7.5 m) and the other in the south basin (Blackstrap Mountain [BSMTN], depth 8 m; Fig. 1).

Field sampling

Sampling was conducted from a boat during the open-water season. During winter, we

accessed the same stations by snowmobile and sampled through holes in the ice (Block et al. 2019). Epilimnetic or surface water was collected for various analyses (Table 1) and $\delta^{18}O$-O_2 stable isotope samples were collected from one to 4 depths per station, depending on water column depth and lake thermal structure that day. Sample details can be found in North et al., (2023). Water samples were collected in acid-washed 20 L carboys, protected from exposure to direct sunlight and temperature fluctuations, and were processed the same evening. On all water bodies, a Yellow Springs Instrument sonde (model 6600 V2) was used to obtain high-resolution vertical profiles of depth, temperature (accuracy = ±0.15 °C, resolution = 0.01 °C), specific conductance (accuracy = ±0.5 %, resolution = 0.001 mS cm^{-1}), O_2 (6150 ROX optical O_2 sensor that was calibrated weekly; accuracy = ±0.1 mg L^{-1}, resolution = 0.01 mg L^{-1}) and Chl *a* (resolution = 0.1 μg L^{-1}) concentrations at each station. Open-water season epilimnion (defined by a change in water temperature of > 0.5 °C m^{-1}) and convective mixed layer thickness (Z_{mix}) were calculated from temperature profiles. We calculated site- and date- specific solar-induced under-ice convective mixed layers on all 4 water bodies defined as the region where the convective Richardson number is ≤ 1 (Pernica et al. 2017).

Physical parameters

Triplicate snow depth measurements were taken on the SK reservoirs with a metric avalanche probe (Z_{snow}; Block et al. 2019). These represented locations where snow had accumulated and where snow had been removed by wind on the ice surface. Triplicate measurements of ice thickness (Z_{ice}) were recorded using a weighted measuring tape. Black ice ($Z_{black\ ice}$; congelation ice) and white ice ($Z_{white\ ice}$; snow ice) thicknesses were differentiated visually. On Lake Simcoe, snow and ice thicknesses ($Z_{snow+ice}$) were recorded from a single hole.

On all 4 water bodies, vertical profiles (0.5 m increments) of photosynthetically active

radiation (PAR) were measured with a Li-Cor scalar (4 pi) or a cosine (2 pi) underwater quantum sensor (Model LI-193SA; Li-Cor, Lincoln, NE, USA). The linear regression of the natural logarithm of irradiance versus depth was calculated from these profiles (vertical attenuation coefficient, K_d; Kirk 1994). To account for the additional effect of attenuation of light through snow and ice, under-ice K_d was determined based on the incident irradiance above ($\bar{E}_0^+$; albedo-corrected) and below (surface PAR) the snow-ice pack with $Z_{snow+ice}$ following the Beer-Lambert equation (K_d = - log(surface PAR / $\bar{E}_0^+$) / $Z_{snow+ice}$). PAR transmission (%) was calculated as surface PAR / $\bar{E}_0^+$. To measure underwater PAR under snow and ice, a model (model I linear regression, R^2_{adj}= 0.972, p< 0.0005, n= 19, $\log_{10}$ transformed data) was developed to convert cosine to scalar readings by multiplying by a factor of 1.85. The PAR sensor was lowered under the ice through a 20.32 cm diameter hole using an articulated arm that positioned the sensor flush with the lower ice surface at a distance one meter from the hole (surface PAR). The integrity of the snow cover was preserved in order to represent realistic transmittance through ice and snow. Albedo was calculated as the ratio of upwelling irradiance ($\bar{E}_u$) to downwelling irradiance ($\bar{E}_d$) collected with the Licor sensor as above at a height of one meter above the snow or ice surface (Belzile et al. 2001). We accounted for the effect of Z_{snow} on albedo with 17 PAR measurements from our SK sites in 2014 (model I linear regression, albedo= [0.017 × Z_{snow}] + 0.654, R^2_{adj}= 0.52, p= 0.001, n= 17). Incident irradiance PAR measured in air ($\bar{E}_{air}$) with a cosine sensor were also adjusted to scalar readings by applying another correction actor (model I linear regression, R^2_{adj}= 0.855, p< 0.0005, n= 16) which involved the multiplication of cosine readings by a factor of 4.25 to yield scalar $\bar{E}_{air}$. Albedo estimates were calculated for each sampling occasion and $\bar{E}_0^+$ values were corrected for derived albedo as follows: $\bar{E}_0^+$= $\bar{E}_{air}$ × (1-albedo). In 2010–2011, mean daily (24-hour) incident irradiance (daily $\bar{E}_0$) was modelled from latitude and day of year

assuming 75 % of theoretical cloud-free values (Kim et al. 2015). In 2013–2014, daily $\bar{E}_0$ was scaled to PAR using a factor of 2.047 from global radiation at a nearby meteorological station (University of Saskatchewan, Saskatoon, SK; http://www.usask.ca/weather/kfarm/data/; Dubourg et al. 2015). For AGP calculations (provided below), daily $\bar{E}_0$ was converted to incident irradiance below the snow/ice ($\bar{E}_0^-$) using the formula $\bar{E}_0^-$ = daily $\bar{E}_0 \times \exp(-K_d \times Z_{snow+ice})$. We derived mean daily mixed layer irradiance ($\bar{E}_{24}$) from water K_d, Z_{mix} (Table 1), and daily $\bar{E}_0$:

$$\bar{E}_{24} = \text{daily } \bar{E}_0 \times (1 - \exp(-1 \times K_d \times Z_{mix})) \times (K_d \times Z_{mix})^{-1} \quad (1)$$

where $\bar{E}_{24}$ describes the amount of light experienced in the convective mixed layer by suspended phytoplankton over a 24-hour period. If the convective mixed layer was absent, under-ice surface PAR was reported as $\bar{E}_{24}$.

We applied physiological light deficiency thresholds to open-water and under-ice phytoplankton communities. Light thresholds for photosynthetic activity (7.6 µmol m^{-2} s^{-1}) and biomass (20 µmol m^{-2} s^{-1}) estimated from sea-ice microalgae by Gosselin et al. (1985) were applied to our under-ice data. During the open-water season, we applied 41.7 µmol m^{-2} s^{-1} (Hecky and Guildford 1984). We also applied the ratio of $\bar{E}_{24}/E_k$ to assess light-deficiency, where E_k is the light saturation parameter derived from fluorometric rapid light curves (RLC, described below). When $\bar{E}_{24} > E_k$, there is theoretically enough light for photosynthesis. Alternatively, when $\bar{E}_{24} < E_k$, phytoplankton may experience light-deficient conditions (Hecky and Guildford 1984). The threshold for light limitation of photosynthesis is an $\bar{E}_{24}/E_k$ ratio of one.

Chemical parameters

Total and dissolved phosphorus (P) and nitrogen (N) forms were measured on epilimnetic water samples. All dissolved nutrient forms were filtered through 0.2 µm pore size polycarbonate filters. In 2010–2011, total P (TP) and total dissolved P (TDP) were analyzed with standard

colorimetric methods (OMOE, 2007). Dissolved reactive P (DRP) was analyzed according to Stainton et al. (1977). In 2013–2014, TP, TDP, and DRP were measured according to Parsons et al. (1984). Total dissolved N (TDN) was measured colorimetrically (OMOE, 2008) in 2010–2011 and via second derivative spectroscopy (Crumpton et al. 1992; Bachmann and Canfield 1996) in 2013–2014. Particulate N (PN) samples were filtered onto pre-combusted (450 °C for 4 h) GFF (nominal pore-size 0.7 μm) filters, which were immediately dried and stored in a desiccator until analysis on a MACRO CNS analyzer (Elementar, Hanau, Germany) in 2010–2011. In 2013–2014, PN samples were collected on pre-combusted quartz filters (GF75, nominal pore size 0.39 μm) and analyzed via an ANCA-GSL sample preparation unit and Tracer 20 mass spectrometer (Europa Scientific). Ammonium (NH_4^+) samples were filtered and analyzed fluorometrically according to Holmes et al. (1999). Nitrate (NO_3^-) samples were filtered and analyzed using a standard colorimetric method (OMOE, 2007) in 2010–2011, and via second-derivative spectroscopy (Crumpton et al. 1992; Bachmann and Canfield 1996) in 2013–2014.

Biological parameters

Samples for Chl *a* analysis were filtered onto glass fiber filters (GFF, nominal pore-size 0.7 μm) and stored in the dark at -20 °C. In 2010–2011, filters were passively extracted with 90 % acetone in the freezer. A fluorometer (Turner Designs 10-AU; Turner Designs, Sunnyvale, California, USA) that was calibrated yearly with pure Chl *a* was used to determine the pheophytin-corrected Chl *a* concentrations (Smith et al. 2005). In 2013–2014, Chl *a* extraction followed Bergmann and Peters (1980) and Webb et al. (1992) with ethanol as a solvent. Samples were corrected for pheophytin using a spectrophotometer (UV-4201 PC, Shimadzu).

In 2010–2011, surface water for particulate organic carbon (POC) was filtered onto pre-combusted (450 °C for 4 h) GFF (nominal pore-size 0.7 μm) filters, which were immediately

dried and stored in a desiccator until analysis. The dried filters were analyzed on a MACRO CNS analyzer (Elementar, Hanau, Germany). In 2013–2014, POC samples were collected on pre-combusted quartz filters (GF75, nominal pore size 0.39 μm), dried and stored until analyzed on an ANCA-GSL sample preparation unit and Tracer 20 mass spectrometer (Europa Scientific). In all years, carbonates were removed from the POC filters by fumigation using concentrated hydrochloric acid (37 %) in a desiccator for 4 h.

Phytoplankton biomass was determined via microscopic counts conducted by Plankton R Us, Winnipeg, Manitoba (Findlay and Kling 1998) and reported as cell wet-weight biomass. Biomass was estimated by approximating cell volume and assuming one as the cellular biomass specific gravity. A minimum of 400 – 600 phytoplankton cells were enumerated using a simple counting chamber fitted to an inverted microscope. Filaments were counted individually and colonies were partially counted.

Metabolism

Three different methods were used to measure under-ice and open-water plankton areal gross production (AGP). Fluorometry (Fluoro) via a Water-PAM fluorometer (Heinz Walz GmbH, Effeltrich Germany) was used to estimate photosynthesis-irradiance (P-E) parameters (light saturation parameter, $E_{K;}$ light-limited slope of the P-E curve, α; maximum relative electron transport rate through PSII, $rETR_{max}$) and derived AGP_F rates on all 4 water bodies. O_2 concentrations and $\delta^{18}O$-O_2 values were used to model AGP-$\delta^{18}O$ rates on all 4 water bodies. On Lake Simcoe only, we used changes in O_2 concentrations via light-dark bottle experiments (LD) to estimate AGP rates. Two methods were used to estimate open-water areal respiration (AR) rates. On all 4 water bodies, O_2 concentrations and $\delta^{18}O$-O_2 values were used to model AR-$\delta^{18}O$ rates. On Lake Simcoe, we applied changes in O_2 concentrations via light-dark bottle

experiments (LD) to estimate AR rates. Areal net production (ANP) rates were determined from the difference between AGP-$\delta^{18}O$ and AR-$\delta^{18}O$ (ANP-$\delta^{18}O$), and between AGP-LD and AR-LD (ANP-LD). The P:R metabolic ratio was also calculated from both the $\delta^{18}O$-O_2 (AGP:AR-$\delta^{18}O$) and LD (AGP:AR-LD) approaches.

A Water-PAM fluorometer controlled by WinControl software (version 3.22) was used to obtain RLCs to estimate P-E parameters and derive AGP_F rates. Prior to obtaining the RLCs, **w**hole-water samples were dark acclimated for 30 min at 20 and 4 °C during the open-water and under-ice sampling seasons, respectively. RLC measurements were obtained in triplicate and corrected for background fluorescence with sample filtrate (0.2 µm pore size polycarbonate filter). RLCs comprised 8, one minute intervals of increasing photon flux density (PFD; range 3–1461 µmol photon m^{-2} s^{-1}). P-E parameters (E_K, α, $rETR_{max}= E_K \times \alpha$) were estimated from each RLC by fitting the equation of Webb et al. (1974) to the Photosystem II (PSII) quantum yield (Φ_{PSII}) as a function of irradiance (Silsbe and Kromkamp 2012):

$$\Phi_{PSII}(E) = \alpha \times E_K \times \left(1 - \mathrm{e}(-\mathrm{E} \times E_K)\right) \times E^{-1} \quad (2)$$

The phytoplankton pigment absorption coefficient was estimated using the quantitative filter technique (Tassan and Ferrari 1995; Silsbe et al. 2012; Petty et al. 2020). AGP_F was calculated with the R package 'phytotools' (Silsbe and Malkin 2015) and integrated through depth and time (Petty et al. 2020).

AGP-$\delta^{18}O$ and AR-$\delta^{18}O$ rates were calculated from the measured O_2 (via sonde) and $\delta^{18}O$-O_2 values. Samples for $\delta^{18}O$-O_2 were collected in pre-evacuated 125 mL serum bottles, capped with butyl blue stoppers, and preserved with sodium azide. Before analysis, a 5 mL helium headspace was added to each bottle by displacing an equivalent volume of water. Headspace and dissolved phases were equilibrated by manual shaking. Analysis of a subsample

of headspace was performed on a modified MicroMass IsoChrom with a 5Å molecular sieve. Precision of the analysis is 0.2 ‰. Samples for $\delta^{18}O\text{-}H_2O$ were collected in triplicate and analyzed on a Los Gatos Liquid-Water Isotope Analyzer, DLT-100. Precision of the measurement is 0.2 ‰. A one mL aliquot was pipetted into a 2 mL vial and sealed with TST septum with cap. Working Standards (purchased from Los Gatos) were run along with samples. Post analysis, data were screened for contamination using LWIA – Spectral Contamination Identifier (software from Los Gatos), followed by correction with LWIA Post Analysis v2.2 software. Certificate of Compliance for the instruments indicate a 0.2 ‰ for $\delta^{18}O\text{-}H_2O$ and 0.6 ‰ for $\delta^{2}H\text{-}H_2O$. Both $\delta^{18}O\text{-}O_2$ and $\delta^{18}O\text{-}H_2O$ results are reported relative to SMOW. We developed a model that extends the steady-state model based on P:R ratios (Quay et al. 1995) to absolute rates (Bocaniov et al. 2015). The deviation from equilibrium saturation conditions of both O_2 and $\delta^{18}O\text{-}O_2$ values is combined with the gas exchange coefficient and Z_{mix} to calculate metabolic rates as:

$$P = \frac{k_{O2,t}}{Z_{mix}} \times \frac{O_2 \times (b-c) - O_{2s} \times (a-c)}{d-c}$$

$$R = \frac{k_{O2,t}}{Z_{mix}} \times \frac{O_2(b-d) - O_{2s}(a-d)}{d-c} \quad (3)$$

where k is the gas exchange coefficient for O_2 at the field temperature (m day^{-1}), C (4)

measured concentration (mmol m^{-3}), O_2s is the 100 % saturation concentration at the field temperature (mmol m^{-3}; Benson and Krause 1984), and a, b, c, and d are:

$$a = \alpha_g \times \alpha_s \times R_{atm} \quad (5)$$

$$b = \alpha_g \times R_{O2} \quad (6)$$

$$c = \alpha_R \times R_{O2} \quad (7)$$

$$d = \alpha_P \times R_{H2O} \quad (8)$$

where α_g is the gas exchange fractionation factor (0.9972; Knox et al. 1992), α_s is the O_2

356 solubility fractionation factor (1.007; Benson et al. 1979), α_R is the respiration fractionation
357 factor (0.985; Kiddon et al. 1993; Quay et al. 1995), α_P is the photosynthesis fractionation factor
358 (1.000; Stevens et al. 1975; Guy et al. 1989, 1993; Helman et al. 2005), R_{atm} is the isotopic ratio
359 of atmospheric O_2 (0.0020523 since $\delta^{18}O$-O_2 is +23.5 ‰; Kroopnick and Craig 1972), R_{O2} is the
360 measured isotopic ratio of O_2, and R_{H2O} is the measured isotopic ratio of H_2O. To estimate k,
361 hourly wind speeds from the previous 7 days at nearby meteorological stations were combined
362 with 2 common windspeed to k_{600} relationships and averaged (Cole and Caraco 1998; Crusius
363 and Wanninkhof 2003). The k_{600} values were converted to the Schmidt number for O_2 at the
364 appropriate field temperature by Schmidt number scaling:

365 $$Sc_{O2,T} = 1800.6 - 120.10 \times T + 3.7818 \times T^2 - 0.047608 \times T^3$$

366 $$k_{O2,T} = k_{600} \times \left(\frac{Sc_{O2,T}}{600}\right)^{\frac{-2}{3}}$$

367 where $Sc_{O2,T}$ is the Schmidt number of O_2 at a given temperature, T (°C), and the exponent -2/3
368 describes the surface conditions of the water (Jähne et al. 1987).

369 Under-ice whole-water metabolism was estimated from changes in O_2 and $\delta^{18}O$-O_2
370 assuming ice cover prevents gas exchange with the atmosphere. Ice-cover dates were determined
371 from the 4 km-resolution IMS Daily Northern Hemisphere Snow and Ice Analysis data (NSIDC:
372 National Snow and Ice Data Center 2008). Metabolic rates were determined by best-fit
373 modelling of the changes in measured O_2 and $\delta^{18}O$-O_2 values since ice-on as:

374 $$\frac{dO_2}{dt} = P - R \qquad (11)$$

375 $$\frac{d\delta^{18}O - O_2}{dt} = P \times R_{H2O} \times \alpha_P - R \times R_{O2} \times \alpha_R \qquad (12)$$

376 Initial conditions for modelling assumed atmospheric equilibrium values for O_2 and $\delta^{18}O$-O_2. To
377 assess the potential variability in rates and include measurement error, the model was run in a

Monte Carlo fashion 100 times per sample (each date-site-depth combination) with randomly chosen initial metabolic rates and error on the measured field values of O_2 and $\delta^{18}O\text{-}O_2$ randomly drawn from the precision around each measurement. In this way, the rates incorporate the uncertainty associated with field measurements. Expecting under-ice metabolic rates to be no greater than maximum open-water values, initial rates were chosen at random from values between zero and the maximum measured open-water rates. Best fits were determined by minimizing the difference between measured field data and model data for both O_2 and $\delta^{18}O\text{-}O_2$ values using the *ode* function in the R package deSolve (Soetaert et al. 2010). Results are summarized as median rates with median absolute deviation as a robust measure of variability since model results were expected to be non-normally distributed. Simulations with 100 and 1000 runs per sample indicate that the difference in medians and median absolute deviation differed by less than 0.1 %. Winter rates are reported at specific depths; epilimnetic rates are from a 2 m water sample. Open-water season epilimnetic rates are reported as averages of discrete samples from above the thermocline.

On Lake Simcoe only, we applied changes in O_2 concentrations via light-dark bottle experiments (LD) to estimate Z_{mix} rates of AGP and AR. Epilimnetic/surface water was used to overfill (by 3 volumes) replicate 300 mL BOD bottles (Pyrex) with Tygon tubing. Randomly selected bottles (3–5) were fixed immediately with Winkler reagents at the beginning of the incubation. O_2 concentrations were measured via Winkler titration on a Mettler Toledo DL50 with a 10 mL burette and a DM-140SC redox electrode (Carignan et al. 1998; Depew et al. 2006b; Bocaniov and Smith 2009). Of the remaining bottles, half were wrapped in 2 layers of aluminum foil (dark treatment) and half were left clear (light treatment) and they were incubated in a modified aquarium under ambient temperature in a temperature-controlled room under

saturating light conditions. Light bottles were incubated for 6 h with 2, 500 W halogen lights, which provided PFD of 300–350 μmol photons m^{-2} s^{-1} as measured with a LiCor cosine underwater quantum sensor. Dark bottles were incubated for 12 h to simulate the natural dark period for plankton and obtain a larger and more easily measured degree of change. After incubations, bottles were removed, fixed with Winkler reagents and subsequently acidified and titrated. The coefficient of variation (CV) of triplicate O_2 determinations, used as a measure of precision, was 0.04%. Gross primary production (GPP) was calculated by subtracting the (negative) rate of change in the dark bottles (respiration, R) from the rate of change in the light bottles (net community production, NCP), assuming equal respiration rates in both dark and light bottles. Dark bottle respiration rates were assumed to be representative of Z_{mix} and AGP-LD was calculated for the euphotic depth (1 % PAR).

Statistical analysis

All assumptions of normality were tested on data subjected to parametric analysis and transformations were applied as needed. Tests of Pearson correlation were employed to assess the relationship between snow depth, ice thicknesses, and surface PAR, as well as AGP_F, $\bar{E}_{24}$, days since ice-on, AGP-$\delta^{18}O$, and AR-$\delta^{18}O$. A 2-way Analysis of Variance (ANOVA) with season (open-water and under-ice) and water body (Blackstrap, Broderick, Diefenbaker, Simcoe) as factors was applied to compare $\bar{E}_{24}$, AGP-$\delta^{18}O$, ANP-$\delta^{18}O$, AR-$\delta^{18}O$, E_k, and $\bar{E}_{24}$:E_k; if the differences were significant, they were followed with *post hoc* Tukey-Kramer tests. The AGP and AR method comparison was conducted via a one-way ANOVA with method as factor, followed by a Tukey *post hoc* for Lake Simcoe AGP. A simple linear regression analysis was used to assess photoacclimation.

Results

Under-ice light environment and controls on productivity

Low winter primary productivity is often attributed to low light conditions. We measured under-ice PAR on all 4 water bodies under ambient snow and ice conditions and then conducted snow removal experiments to assess the impact on PAR at the ice-water interface. The only significant predictor of under-ice PAR was snow depth (r= -0.641, p< 0.0005, n= 39). There was no relationship between under-ice PAR and total ice thickness (r= -0.153, p= 0.353, n= 39), nor white ice thickness (r= -0.02, p= 0.929, n= 22), nor black ice thickness (r= -0.236, p= 0.278, n= 23). Under ice cover, PAR values can be assessed for light deficiency for phytoplankton according to a light intensity threshold for biomass accrual (<20 μmol m^{-2} s^{-1}; Gosselin et al. 1985) and a lower threshold for photosynthesis (<7.6 μmol m^{-2} s^{-1}; Gosselin et al. 1985). Under ambient snow cover, under-ice PAR was deficient for biomass accrual 51 % of the 39 times measured and 26 % of the time it was light deficient for photosynthesis. After snow removal, there was a 67 % increase in the under-ice PAR (Fig. 2), resulting in deficiency for biomass accrual occurring 12 % of the 17 times measured, and only 6 % were deficient for photosynthesis if snow cover is absent.

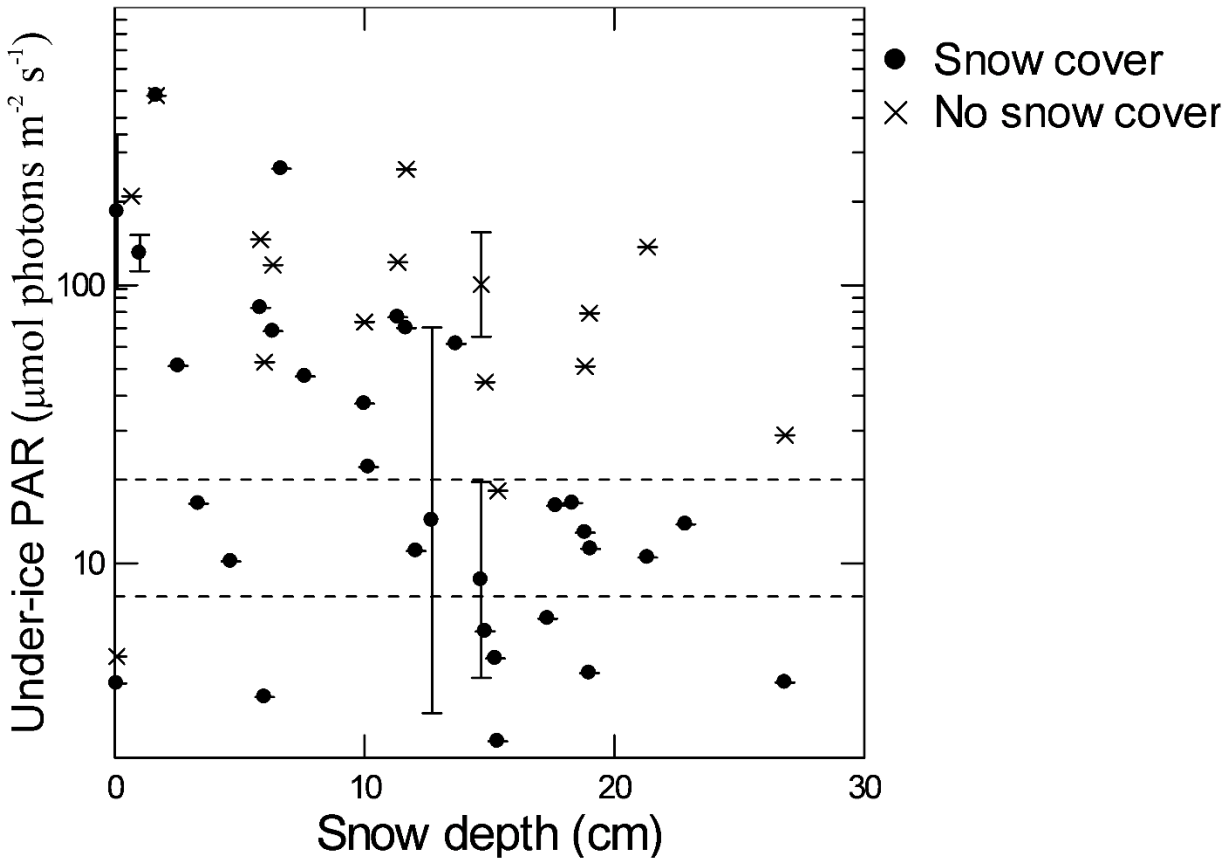

Figure 2. Impact of snow removal on under-ice photosynthetically active radiation (PAR). Shown are the mean and standard error of PAR readings (note log scale) at the ice-water interface as a function of snow depth for all water bodies and dates. Black circles represent under-ice PAR with ambient snow conditions, and "x"s show measurements taken after snow was physically removed. The top horizontal line at 20 μmol m^{-2} s^{-1} is the light intensity threshold for under-ice biomass accrual and the bottom horizontal line at 7.6 μmol m^{-2} s^{-1} is the light intensity threshold for photosynthesis (Gosselin et al. 1985).

Surface or under-ice PAR is not entirely representative of the water column where phytoplankton are growing and photosynthesizing. $\bar{E}_{24}$ is used to represent the amount of light in the convective mixed layer over a 24-hour period and allows for comparison between open-water

and under-ice seasons (Fig. 3; Tables 1 & 2). The highest $\bar{E}_{24}$ values (~ 92 µmol m^{-2} s^{-1}) occurred on Blackstrap and Broderick reservoirs during the open-water season and on Lake Simcoe under-ice. The lowest $\bar{E}_{24}$ values (~ 20 µmol m^{-2} s^{-1}) occurred on Blackstrap and Broderick reservoirs under-ice (Fig. 3; Table 1). Under-ice $\bar{E}_{24}$ was consistently (although not significantly) lower than open-water, with the exception of Lake Simcoe, where we attribute the high under-ice $\bar{E}_{24}$ to the absence of snow cover resulting in shallow convective mixing depths (Pernica et al. 2017). Lake Simcoe under-ice $\bar{E}_{24}$ was significantly higher than the 3 Saskatchewan reservoirs (Table 2).

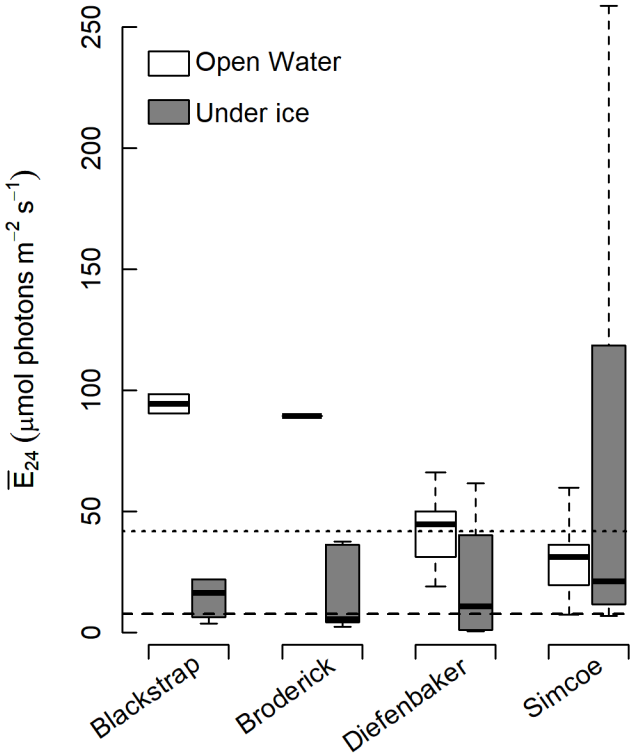

Figure 3. Comparison of the mean light experienced in the convective mixed layer by suspended phytoplankton over a 24-hour period ($\bar{E}_{24}$) between open-water (open boxes) and under-ice (black boxes) for each of the 4 water bodies. Boxplots display the median of $\bar{E}_{24}$ with the first, and third quartiles, and whiskers indicate the minimum and maximum values. The top horizontal

463 line at 41.7 μmol m^{-2} s^{-1} is the open-water light threshold (Hecky and Guildford 1984) and the
464 bottom horizontal line at 7.6 μmol m^{-2} s^{-1} is the under-ice light threshold (Gosselin et al. 1985).

465 **Table 2.** Two-way Analysis of Variance (ANOVA) and Tukey-Kramer *post hoc* comparisons
466 between season (open-water and under-ice) and water body (Blackstrap, Broderick, Diefenbaker,
467 Simcoe) for physical and biological parameters (Table 1). *Post-hoc* tests were conducted if
468 ANOVA factors were identified as significant ($p < 0.05$). The letters for the *post-hoc* comparison
469 indicate statistical significance ($p < 0.05$); the relationship between identical letters is not
470 statistically significant, whereas the relationship between different letters is significant. $\bar{E}_{24}$, mean
471 daily mixed layer irradiance; AGP, Areal Gross Productivity; ANP, Areal Net Productivity; AR,
472 Areal Respiration; E_k, light saturation parameter; α, light-limited slope of the P-E curve.

473

Parameter				***Post-hoc* test**		***Post-hoc* test**			
				Open-water	Under-ice	Blackstrap	Broderick	Diefenbaker	Simcoe
$\bar{E}_{24}$	season		$F_{1,125}$=18.724, p<0.0005						
	water body		$F_{3,125}$=2.433, p=0.068						
	interaction		$F_{3,125}$=8.700, p<0.0005						
		open-water				a	a	a	a
		under-ice				ac	ab	a	c
		Blackstrap		a	a				
		Broderick		a	a				
		Diefenbaker		a	b				
		Simcoe		a	a				
AGP-$\delta^{18}O$	season		$F_{1,91}$=369.225, p<0.0005						
	water body		$F_{3,91}$=1.776, p=0.157						
	interaction		$F_{3,91}$=7.903, p<0.0005						

		open-water				a	ab	ab	b
		under-ice				a	a	a	a
		Blackstrap		a	b				
		Broderick		a	b				
		Diefenbaker		a	b				
		Simcoe		a	b				
ANP-$\delta^{18}O$	season		$F_{1,90}$=39.175, p<0.0005						
	water body		$F_{3,90}$=2.108, p=0.105						
	interaction		$F_{3,90}$=8.287, p<0.0005						
		open-water				a	ab	ab	b
		under-ice				a	b	a	a
		Blackstrap		a	b				
		Broderick		a	b				
		Diefenbaker		a	a				
		Simcoe		a	a				
AR-$\delta^{18}O$	season		$F_{1,91}$=200.805, p<0.0005						

	water body		$F_{3,91}$=17.172, p<0.0005						
	interaction		$F_{3,91}$=3.321, p=0.023						
		open-water				a	a	a	a
		under-ice				a	a	b	b
		Blackstrap		a	b				
		Broderick		a	a				
		Diefenbaker		a	b				
		Simcoe		a	b				
AGP:AR-$\delta^{18}O$	season		$F_{1,89}$=21.778, p<0.0005						
	water body		$F_{3,89}$=9.296, p<0.0005						
	interaction		$F_{3,89}$=16.180, p<0.0005						
		open-water				a	a	a	a
		under-ice				a	a	b	b
		Blackstrap		a	b				
		Broderick		a	b				

		Diefenbaker		a	a				
		Simcoe		a	a				
E_k	season		$F_{1,133}$=9.180, p=0.003						
	water body		$F_{3,133}$=28.102, p<0.0005						
	interaction		$F_{3,133}$=0.522, p=0.668						
		open-water				a	ab	a	b
		under-ice				a	a	a	b
		Blackstrap		a	a				
		Broderick		a	a				
		Diefenbaker		a	b				
		Simcoe		a	b				
α	season		$F_{1,133}$=0.576, p=0.449						
	water body		$F_{3,133}$=0.233, p=0.873						
	interaction		$F_{3,133}$=0.925, p=0.431						
$\bar{E}_{24}$:E_k	season		$F_{1,116}$=2.673, p=0.105						
	water body		$F_{3,116}$=10.235, p<0.0005						

interaction		$F_{3,116}$=4.543, p=0.005						
	open-water				a	a	a	a
	under-ice				a	a	a	b
	Blackstrap	a	a					
	Broderick	a	a					
	Diefenbaker	a	a					
	Simcoe	a	a					

474

475 AGP_F is influenced by $\bar{E}_{24}$ under-ice, but not during the open-water season (Fig. 4). Year-
476 round, there is a positive, significant relationship between AGP_F and $\bar{E}_{24}$ (R= 0.265, p= 0.003).
477 During the open-water season, this relationship weakens (R= -0.083, p= 0.434), indicating it is
478 strongly driven by under-ice measurements (R= 0.311, p= 0.078). The relationship between
479 AGP-$\delta^{18}O$ and $\bar{E}_{24}$ is also positive and significant year-round (R= 0.247, p= 0.020), but displays
480 the opposite seasonal relationship as AGP_F, wherein open-water AGP-$\delta^{18}O$ rates are dictated by
481 $\bar{E}_{24}$ (R= 0.524, p<0.0005), but there is no relationship under-ice (R= 0.337, p= 0.107).
482 The maximum and minimum individual $\bar{E}_{24}$ values occur under-ice (Fig. 4, Table 1), with
483 the maximum AGP_F occurring on Lake Diefenbaker during the open-water season, and the
484 minimum under-ice on Blackstrap reservoir. During the open-water season on all 4 water bodies,
485 74 % of the individual $\bar{E}_{24}$ values indicated light deficiency (<41.7 µmol m^{-2} s^{-1}, Hecky and
486 Guildford 1984) while under-ice, 29 % indicated light deficiency (<7.6 µmol m^{-2} s^{-1}, Gosselin et
487 al. 1985; Fig. 4).

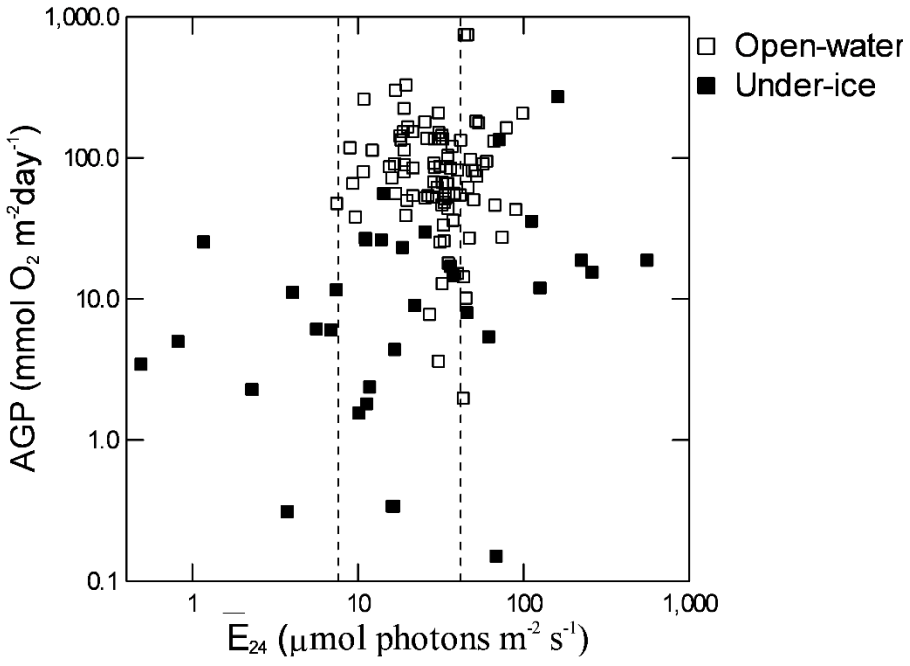

488

Figure 4. The relationship between fluorometrically-derived areal gross production (AGP) rates and mean light ($\bar{E}_{24}$), differentiated by open-water and under-ice seasons for all study water bodies. The left vertical line at 7.6 μmol m^{-2} s^{-1} is the under-ice light threshold (Gosselin et al. 1985) and the right vertical line at 41.7 μmol m^{-2} s^{-1} is the open-water light threshold (Hecky and Guildford 1984).

Dissolved inorganic P and N concentrations can also limit productivity. Under-ice DRP, NH_4^+, and NO_3^- concentrations were 10x, 3x, and 59x higher than the open-water concentrations, respectively (Table 1). Under-ice DRP concentrations (mean= 0.18 μmol L^{-1}, Table 1) and dissolved inorganic nitrogen ($NH_4^+ + NO_3^-$) concentrations (mean= 9.7 μmol L^{-1}, Table 1) were sufficient relative to dissolved inorganic nutrient deficiency thresholds (DRP, 0.10 μmol L^{-1}, DIN, 7.1 μmol L^{-1}; Chorus and Spijkerman 2020).

Spatial and temporal variability in metabolism

Comparison of AGP, AR, ANP and the P:R ratio allows us to determine if water bodies are net autotrophic (P:R> 1) and dominated by primary productivity, or net heterotrophic (P:R< 1) and dominated by respiration. The $\delta^{18}O$-O_2 approach is the only method with both production and respiration rates in all 4 water bodies; this robust dataset was used to examine spatial (between water bodies and vertical [under-ice]) and temporal (open-water/under-ice and days since ice-on) metabolic rates. During the open-water season, the mean AGP-$\delta^{18}O$ rates for all 4 water bodies (35.8 mmol O_2 m^{-2} day^{-1}) is 81x higher than the mean under-ice rates (0.4 mmol O_2 m^{-2} day^{-1}; Table 3). Open-water mean AR-$\delta^{18}O$ rates for all 4 water bodies (32.1 mmol O_2 m^{-2} day^{-1}) is 8x higher than the mean under-ice rates (4.1 mmol O_2 m^{-2} day^{-1}; Table 3).

510 **Table 3.** Method comparison between open-water and under-ice approaches to measuring areal gross production (AGP) and areal
511 respiration (AR) rates differentiated by water body. AGP rates are derived from fluorometric (Fluoro), $\delta^{18}O$, and LD methods. AR
512 rates are derived from $\delta^{18}O$ and LD methods. Note that LD methods were only employed on Lake Simcoe. Data were transformed and
513 then analyzed with a one-way ANOVA with method as factor and Tukey-Kramer *post hoc* comparisons (Simcoe AGP only). Bolded
514 values are significantly different ($p<0.05$) and the higher rates are italicized. AGP and AR values are in units of mmol O_2 m^{-2} day^{-1}.
515 NA, Not Applicable; ANP, LD, light-dark bottle experiments; AGP, Areal Gross Productivity; AR, Areal Respiration. **n* = 1.

	Blackstrap		**Broderick**		**Diefenbaker**		**Simcoe**	
	AGP	AR	AGP	AR	AGP	AR	AGP	AR
Open-water								
F-value	$F_{1,1}$=4.634	NA	NA*	NA	$F_{1,13}$=3.057	NA	$F_{2,164}$=25.118	$F_{1,99}$=70.553
p-value	0.277				0.104		<0.0005	<0.0005
Method								
Fluoro	207.2		43.0		203.9		***84.9***	
$\delta^{18}O$	116.3	96.3	73.5	62.6	49.7	43.2	31.9	***29.0***
LD							29.5	**10.1**

Under-ice								
F-value	$F_{1,14}$=5.237	NA	$F_{1,9}$=40.190	NA	$F_{1,15}$=43.606	NA	$F_{2,42}$=15.984	$F_{1,25}$=18.109
p-value	0.038		<0.0005		<0.0005		<0.0005	<0.0005
Method								
Fluoro	***32.6***		***10.2***		***18.0***		***29.5***	
$\delta^{18}O$	**0.1**	4.8	**0.2**	11.7	**0.5**	0.5	0.9	**0.7**
LD							1.1	***10.6***

516

517 During the open-water season, all the water bodies were net autotrophic with AGP-$\delta^{18}O$
518 rates ranging from 116.3 (Blackstrap) to 31.9 mmol O_2 m^{-2} day^{-1} (Simcoe; Table 3; Fig. 5A).
519 ANP-$\delta^{18}O$ was significantly higher on Blackstrap (20.0 mmol O_2 m^{-2} day^{-1}) than Simcoe (2.9
520 mmol O_2 m^{-2} day^{-1}), while AR-$\delta^{18}O$ rates were not different between water bodies (Tables 1, 2 &
521 3; Fig. 5A). Under ice, Blackstrap and Broderick were heterotrophic, while Diefenbaker and
522 Simcoe were autotrophic (Table 1, Fig. 5B, Table 4). AGP-$\delta^{18}O$ rates were low (0.4 mmol O_2 m^{-2}
523 day^{-1} mean for all water bodies) and not significantly different between water bodies (Tables 2 &
524 3; Fig. 5B). Under-ice ANP-$\delta^{18}O$ rates were significantly lower on Broderick (-12.9 mmol O_2 m^{-2}
525 day^{-1}) than the other water bodies (mean of -1.7 mmol O_2 m^{-2} day^{-1}). AR-$\delta^{18}O$ was significantly
526 higher on Blackstrap and Broderick (mean of 8.2 mmol O_2 m^{-2} day^{-1}) than Diefenbaker and
527 Simcoe (mean of 0.6 mmol O_2 m^{-2} day^{-1}; Tables 2 & 3; Fig. 5B). Open-water AGP-$\delta^{18}O$ was
528 significantly higher than under-ice for all 4 water bodies (Table 4). Open-water ANP-$\delta^{18}O$ was
529 significantly higher on Blackstrap and Broderick than under-ice rates; seasonal rates were similar
530 on Diefenbaker and Simcoe. Open-water AR-$\delta^{18}O$ was significantly higher than under-ice for all
531 water bodies with the exception of Broderick (Tables 2, 3 & 4; Fig. 5).

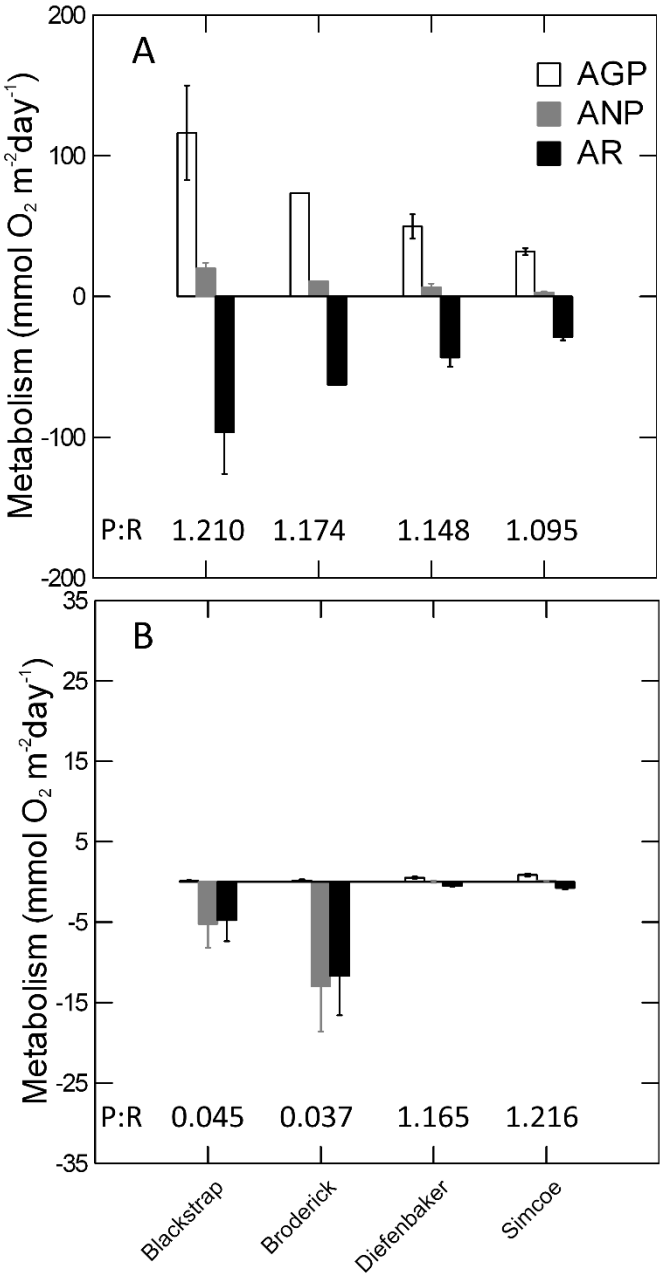

532

533 **Figure 5.** Comparison of metabolic rates between the 4 study water bodies. A) Open-water areal
534 gross production (AGP- $\delta^{18}O$), areal net production (ANP- $\delta^{18}O$), and areal respiration (AR-
535 $\delta^{18}O$) rates. B) Under-ice AGP- $\delta^{18}O$, ANP- $\delta^{18}O$, and AR- $\delta^{18}O$ rates. The AGP:AR- $\delta^{18}O$ (P:R)
536 ratios for each water body and both seasons are shown as text. Bars display the mean and
537 standard error of the metabolic rates. Note the different y-axis scales.

538 **Table 4.** Literature review of open-water (OW) and under-ice (UI) areal gross production (AGP) and areal respiration (AR) ratios. For
539 different approaches to measuring AGP and AR on the same water samples, ranges (minimum-maximum) are reported, otherwise,
540 shown are the means. Ratios were collected directly from text or estimated via table values or by digitizing figures. Given the diversity
541 of methods and units and thus, the inherent assumptions that must be made to convert between methods, we chose to report rates as
542 ratios and avoided comparing our absolute rates with published rates.

Water body	**Location**	**OW:UI AGP**	**OW:UI AR**	**OW AGP:AR**	**UI AGP:AR**	**Year-round AGP:AR**	**Citation**
Blackstrap	Canada	6–1163	20	1.2	0.0	0.3	This study
Broderick	Canada	4–368	5	1.2	0.0	0.2	This study
Diefenbaker	Canada	11–99	86	1.1	1.2	1.2	This study
Simcoe	Canada	3–35	1–41	1.1–12.6	0.5–1.2	1.1–8.2	This study
Simcoe	Canada	5					Kim et al. 2015
Simoncouche	Canada	73					Grosbois et al. 2020
Ontario	Canada/US	2.5					Glooschenko et al. 1974
Michigan	Canada/US	~1					Biddanda and Cotner 2002
Erie	Canada/US	3					Depew et al. 2006b

Erie	Canada/US	2	Saxton et al. 2012
Erie	Canada/US	~1	D'souza 2012
Sylvan	US	6	Wetzel 1966
Lawrence	US	6	Wetzel 2001
Goose	US	5	Wetzel 1966
Char	US	2	Kalff and Welch 1974
Wintergreen	US	2	Wetzel 2001
Santo Parmense	Italy	6	Camurri et al. 1976; Ferrari 1976
Võrtsjärv	Estonia	4	Noges and Noges 1999
Druzhby	Antarctica	0.3	Henshaw and Laybourn-Parry 2002
Balaton	Hungary	6	Dokulil et al. 2014
Neusiedler See	Hungary	6	Dokulil et al. 2014
Haruna	Japan	~1	Maeda and Ichimura 1973
Meretta	Canada	~1	Kalff and Welch 1974

Sunapee	US	0.8				Brentrup et al. 2020
Calvert	US		1.1	0.6	0.8	Gammons et al. 2013
Georgetown	US		1.0	0.6	0.8	Gammons et al. 2014
Winnipeg	Canada		0.8		0.9	Wassenaar 2012

543

Under-ice AGP:AR-$\delta^{18}O$ decreased with depth in Lakes Diefenbaker and Blackstrap (Fig. 6). While the P:R ratio is less than one throughout the water column on Blackstrap, Broderick, and Diefenbaker, Lake Simcoe is net autotrophic during the winter at all sampling depths (Figs 6 & 7), likely driven by high $\bar{E}_{24}$ values (Fig. 3). Just under the ice surface, Lake Diefenbaker is also net autotrophic, but P:R was usually less than one below 7.5 m depth (Fig. 6). In Blackstrap and Broderick, it is the AR-$\delta^{18}O$ that is increasing with depth. From the surface to 6 m, AR-$\delta^{18}O$ increased from 0.5 to 25.9 mmol O_2 m^{-2} day^{-1} in Blackstrap, and from zero to 59.7 mmol O_2 m^{-2} day^{-1} in Broderick. In Diefenbaker, the decrease in AGP:AR-$\delta^{18}O$ with depth is primarily driven by decreases in AGP-$\delta^{18}O$, which is as high as 1.1 mmol O_2 m^{-2} day^{-1} at the surface, and zero below 20 m. AR-$\delta^{18}O$ is consistently zero throughout the water column in both Diefenbaker and Simcoe. In Simcoe, AGP-$\delta^{18}O$ rates are also consistent with depth, only ranging from 0.4–0.7 mmol O_2 m^{-2} day^{-1} throughout the water column. In Simcoe, the average under-ice $\bar{E}_{24}$ value of 40.6 (range: 6.9–555.6 µmol m^{-2} s^{-1}) is significantly higher than Diefenbaker (mean: 42.5, range: 0.5–223.0 µmol m^{-2} s^{-1}) and Broderick (mean: 29.2, range: 2.3–89.5 µmol m^{-2} s^{-1}; Tables 1 & 2, Fig. 3) and well above the light deficiency threshold (7.6 µmol m^{-2} s^{-1}, Gosselin et al. 1985; Fig. 3). The deep euphotic zone under-ice in Lake Simcoe appears to facilitate photosynthesis down to depths as deep as 35 m.

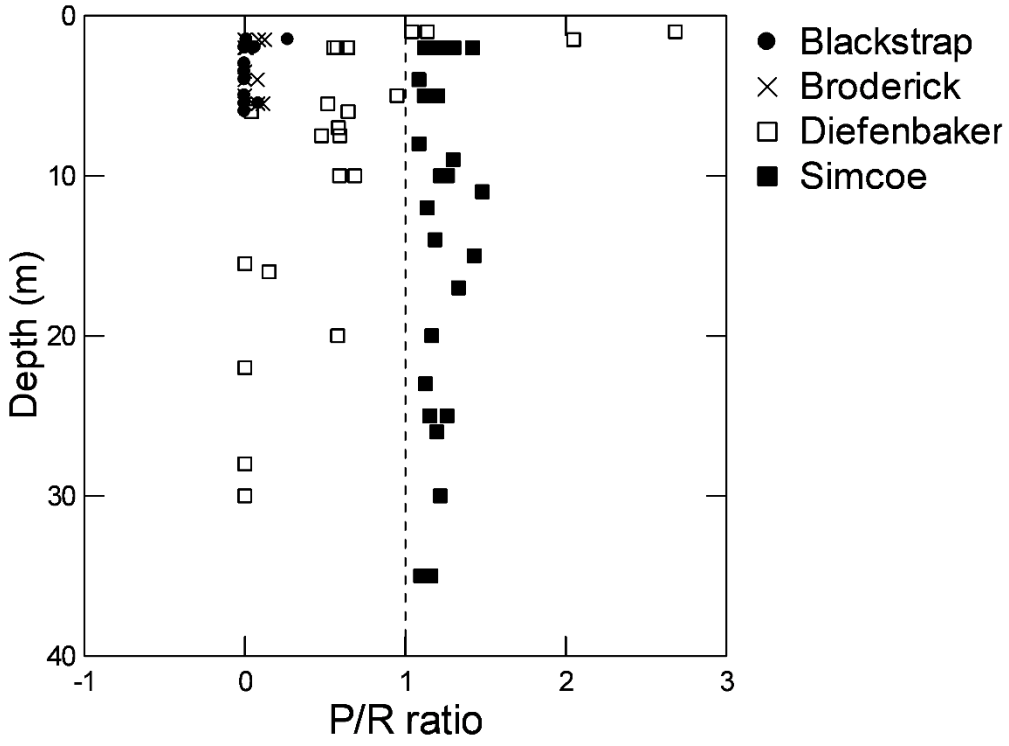

Figure 6. The vertical distribution of the under-ice AGP:AR- $\delta^{18}O$ (P:R) ratios differentiated by water body. Symbols left of the vertical line at one indicate heterotrophy, while symbols on the right of the line indicate autotrophy.

All of the water bodies were sampled multiple times over the winter, allowing us to examine relationships between days since ice-on and metabolism (Fig. 7). There were no relationships between AGP-$\delta^{18}O$ nor AR-$\delta^{18}O$ and days since ice-on for any of the water bodies; however, on Lake Simcoe, there was a negative relationship between days since ice on and snow depth (r= -0.917, p= 0.007, n= 9). Wind-swept conditions on a large lake such as Simcoe result in negligible snow cover at the end of the winter (Table 1). On the last day of safe sampling on the ice at station K42 of Lake Simcoe (Fig. 1) on March 14th 2011, we recorded the maximum under-ice Chl *a* concentration (13.1 µg L^{-1}; Table 1) that extended 15 m deep in the water column (Fig. 5 in Pernica et al. 2017). Surface water phytoplankton biomass was 1,577.00 mg m^{-}

574 ^{3} and was composed primarily of a small centric diatom (*Stephanodiscus*). This Chl *a* peak
575 corresponded with the maximum under-ice fluorometric and light-dark AGP rates for Lake
576 Simcoe (AGP_F: 271.7, AGP-LD: 8.0 mmol O_2 m^{-2} day^{-1}; Table 3). The AGP-$\delta^{18}O$ rates on this
577 date and station (1.2 mmol O_2 m^{-2} day^{-1}) were slightly lower than the maximum of 1.9 mmol O_2
578 m^{-2} day^{-1} (Table 3).

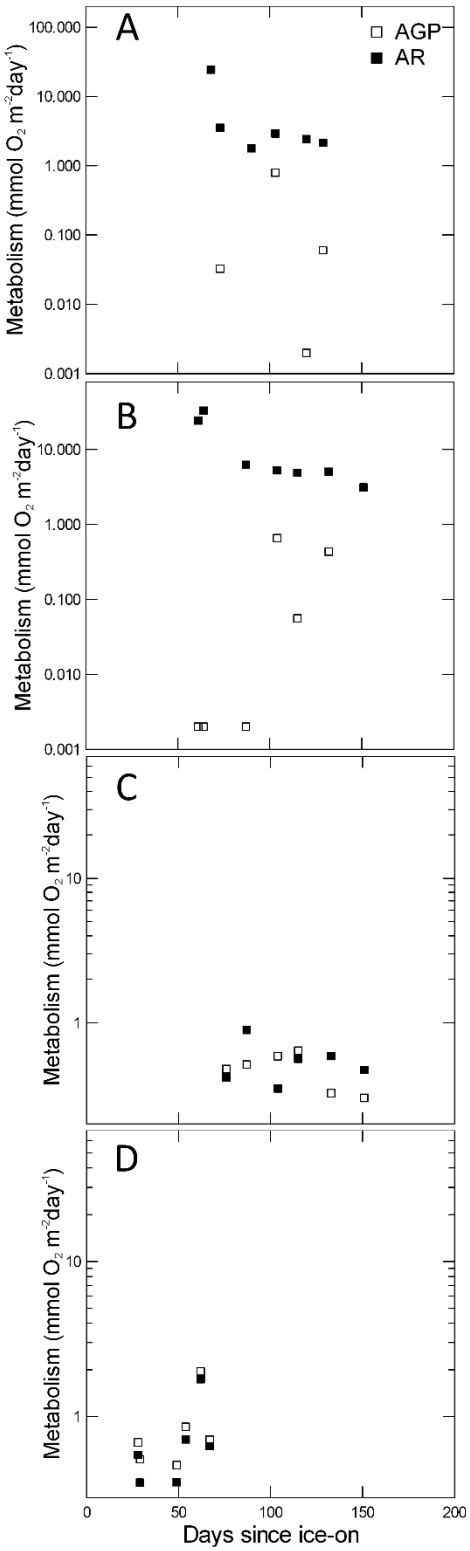
A
B
C
D
AGP
AR
Metabolism (mmol O2 m-2day-1)
100.000
10.000
1.000
0.100
0.010
0.001
10
1
0
50
100
150
200
Days since ice-on

579

Figure 7. Under-ice metabolic rates over the winter season (days since ice-on). Shown are individual rates of areal gross production (AGP- $\delta^{18}O$) and areal respiration (AR- $\delta^{18}O$) from 2 m water samples. A) Blackstrap, B) Broderick, C) Diefenbaker, D) Simcoe.

Comparison of production and respiration methods

We applied 3 different methods for measuring rates of AGP and AR (Table 2). The ratio between the different open-water AGP methods ranged from 1.2 (LD: $\delta^{18}O$, 0.1–3.6, *n*= 23) to 4.3 (Fluoro: $\delta^{18}O$, 0.1–24.8, *n*= 60) to 7.3 (Fluoro:LD, 1.2–40.5, *n*= 22; Table 3). The methodological differences between AGP_F and AGP-$\delta^{18}O$ were insignificant for the Saskatchewan reservoirs. On Lake Simcoe, we also used the light-dark method to measure AGP; the AGP_F method yielded significantly higher rates than both AGP-$\delta^{18}O$ and AGP-LD methods (Table 3). Ratios of AR during the open water season were 0.5 (LD: $\delta^{18}O$, 0.0–3.3, *n*= 35). Since only one AR method was applied during the open-water season on the Saskatchewan reservoirs, the only comparison possible is between AR-$\delta^{18}O$ and AR-LD methods on Lake Simcoe. The AR-$\delta^{18}O$ approach yielded significantly higher rates than the AR-LD during the open-water season on Lake Simcoe (Table 3).

Estimates of under-ice AGP ratios ranged from 1.5 (LD: $\delta^{18}O$, 0.0–6.5, *n*= 9) to 399.0 (Fluoro: $\delta^{18}O$, 0.4–4,507.2, *n*= 25) to 1,127.9 (Fluoro:LD, 5.0–1,1746.7, *n*= 13; Table 2). All of the differences between AGP_F and AGP-$\delta^{18}O$ were significant, with AGP_F being consistently higher on every water body. On Lake Simcoe, AGP_F was also significantly higher than AGP-LD (Tables 2 & 3). Under-ice AR ratios on Lake Simcoe were 12.0 (LD: $\delta^{18}O$, 1.3–47.2, *n*= 9), with AR-LD having significantly higher rates than AR-$\delta^{18}O$ (Table 3). On Blackstrap and Diefenbaker, we also estimated under-ice respiration rates using continuous O_2 sensors and the

602 free-water approach (Solomon et al. 2013). AR ratios ($\delta^{18}O$:free-water) were 0.5 and 0.007,
603 respectively (Supplemental Information).
604 *Physiological light response variables*
605 The P-E parameter, E_k, is the light saturation parameter and can serve as an indicator of
606 the phytoplankton community's capacity for light. The open-water E_k values on Lake Simcoe
607 were significantly lower than both Blackstrap and Diefenbaker, and under ice they were
608 significantly lower than all of the SK reservoirs (Tables 1 & 2). Open-water and under-ice E_k
609 values were similar on Blackstrap and Broderick but were significantly higher during the open-
610 water season than under-ice on Lakes Diefenbaker and Simcoe (Tables 1 & 2). The E_k values can
611 be compared to the light intensity thresholds for the open-water season (<41.7 μmol m^{-2} s^{-1};
612 Hecky and Guildford 1984) and under-ice (<7.6 μmol m^{-2} s^{-1}; Gosselin et al. 1985). During the
613 open-water season, E_k values on Blackstrap, Broderick, Diefenbaker, and Simcoe were 17, 8, 11,
614 and 4 x higher, respectively, than the 41.7 μmol m^{-2} s^{-1} threshold (Hecky and Guildford 1984).
615 Under ice, E_k values on Blackstrap, Broderick, Diefenbaker, and Simcoe were 47, 41, 30, and 10
616 x higher, respectively, than the 7.6 μmol m^{-2} s^{-1} threshold (Gosselin et al. 1985). Across all water
617 bodies, under-ice E_k is 32x higher than the threshold, and open-water E_k is 10x times higher than
618 the threshold, suggesting that if light conditions improve, winter phytoplankton will respond ~3x
619 more strongly than summer phytoplankton communities. The light-limited slope of the P-E curve
620 (α) was similar across water bodies and between seasons (Tables 1 & 2).
621 The ratio of $\bar{E}_{24}/E_k$ can also serve as an indicator of light deficiency with a threshold of
622 one (Hecky and Guildford 1984). This ratio is <1 consistently for all water bodies and both
623 seasons with the exception of Lake Simcoe under-ice, which has a significantly higher ratio than
624 the SK reservoirs (Tables 1 & 2). The $\bar{E}_{24}/E_k$ ratios were similar between seasons.

625 *Photoacclimation*

626 Phytoplankton acclimate to lower light by increasing their light harvesting pigments such
627 as Chl *a* (Arrigo et al. 2010). Given the significant differences in light between water bodies and
628 seasons (Tables 1 & 2, Fig. 3), we are cognizant that Chl *a* may not consistently serve as a proxy
629 for phytoplankton biomass. We measured both phytoplankton biomass and particulate organic C
630 (POC) and assessed their relationships to Chl *a*; photoacclimation could be occurring if there is a
631 weak relationship between Chl *a* and biomass or POC. There was never a relationship between
632 Chl *a*, biomass, nor POC for Blackstrap and Broderick under-ice (Table 5). In Lake Diefenbaker,
633 Chl *a* and POC were significantly, positively related during the open-water season, but not under
634 ice. There was, however, a significant positive relationship between Chl *a* and biomass, and POC
635 and biomass, indicating photoacclimation may not be occurring under-ice on Lake Diefenbaker.
636 In Lake Simcoe, while the relationship between Chl *a* and POC was strong during the open-
637 water season, it weakened during the winter (Table 5). The poor under-ice relationships between
638 Chl *a*, phytoplankton biomass, and POC indicates that photoacclimation is occurring under the
639 low light conditions of the under-ice season; therefore, Chl *a* is an unsuitable proxy for
640 phytoplankton biomass in the winter.

641 **Table 5.** Linear regressions between Chlorophyll *a* (Chl *a*), Particulate Organic Carbon (POC), and phytoplankton biomass (Phyto)
642 differentiated by water body and open-water and ice-covered seasons. Relationships where $n < 3$ were excluded. Significant
643 relationships are identified with bolded R^2_{adj} values.

Water body	**Season**		Chl *a*	POC
Blackstrap	Under-ice	POC	R^2_{adj}= 0.000, p= 0.968, n= 7	
		Phyto	R^2_{adj}= 0.000, p= 0.386, n= 8	R^2_{adj}= 0.000, p= 0.726, n= 7
Broderick	Under-ice	POC	R^2_{adj}= 0.243, p= 0.296, n= 4	
		Phyto	R^2_{adj}= 0.000, p= 0.775, n= 4	R^2_{adj}= 0.000, p= 0.655, n= 4
Diefenbaker	Open-water	POC	R^2_{adj}= **0.630**, p= 0.001, n= 12	
	Under-ice	POC	R^2_{adj}= 0.087, p= 0.245, n= 8	
		Phyto	R^2_{adj}= **0.518**, p= 0.027, n= 8	R^2_{adj}= **0.434**, p= 0.045, n= 8
Simcoe	Open-water	POC	R^2_{adj}= **0.174**, p< 0.0005, n= 88	
	Under-ice	POC	R^2_{adj}= 0.140, p= 0.058, n= 20	

644

Discussion

Year-round P:R ratios are close to unity, with autotrophy dominating in the open-water season and heterotrophy under ice. Under-ice AGP is strongly influenced by light, with lower production and respiration than during the open-water season. The depth of snow cover dictates the under-ice PAR (Pernica et al. 2017). On Lake Simcoe, snow depth decreased over the winter, resulting in the highest AGP rates on the last date of winter sampling. This coincided with the maximum Chl *a* concentration. When the snow is removed, there is a 67 % increase in under-ice PAR; the winter phytoplankton communities appear to be physiologically poised to respond to increases in light, with potential increases in productivity. While open-water and under-ice $\bar{E}_{24}$ values were not significantly different, half of the time under-ice PAR was below the light deficiency threshold for phytoplankton. Changes in under-ice light, therefore, will have a profound influence on under-ice metabolism, with consequent effects on year-round lake function. Given the overriding effect of snow on PAR, snow appears to be a keystone winter variable, influencing in-lake metabolism.

How do under-ice rates of productivity and respiration compare with open-water rates?

Open-water AGP in our water bodies across the 3 methods ranged from 3–1163x higher than the under-ice rates (Table 4). Comparison of summer and winter production rates on the Laurentian Great Lakes (summarized in Ozersky et al. [2021]) ranged from no differences on Lakes Michigan (Biddanda and Cotner 2002) and Erie (D'souza 2012) to 3x higher in the eastern basin of Lake Erie (Depew et al. 2006a). The open-water to under-ice AGP ratio varies from less than one (0.3) in an Antarctic lake (Henshaw and Laybourn-Parry 2002) to 73 in a Canadian lake (Grosbois et al. 2020) with the average ratio (excluding this study) of 7 (Table 4). Open-water AR for our 4 water bodies ranged (combining the 2 methods) from 1–86x higher than the under-

668 ice rates (Table 4). The opposite was found in an oligotrophic lake, where under-ice respiration
669 was 1.2 times higher than summer respiration (Brentrup et al. 2021). During the open-water
670 season, the AGP:AR ratio was consistently higher than unity in our study systems, averaged
671 around one for 2 US lakes (Gammons et al. 2013, 2014), and was less than one on Canadian
672 Great Lake Winnipeg (Wassenaar 2012; Table 4). Under ice, our AGP:AR ratio ranged from
673 zero to 1.2, with an average ratio of 0.6 for 2 US lakes (Gammons et al. 2013, 2014b; Table 4),
674 indicating heterotrophy was dominant in the winter. Net heterotrophy was also reported for Lake
675 Tovel (Italy) with the use of high frequency under-ice O_2 sensors (Obertegger et al. 2017).
676 The year-round AGP:AR ratio ranges from 0.2 to 8.2 for our study systems, while the
677 only 3 other lakes with comparable ratios average less than one (0.8; Table 4). Given that our
678 ratios averaged around one, this likely is a delicate balance that can shift from year-to-year,
679 depending on the length and severity of winter conditions and subsequent light environment. In
680 Canadian water bodies, including a Saskatchewan reservoir (Finlay et al. 2019), year-round CO_2
681 budgets revealed positive net annual CO_2 fluxes, indicating heterotrophy. The under-ice CO_2
682 accumulation accounted for 3–80 % (Ducharme-Riel et al. 2015) and 31–64 % (Finlay et al.
683 2019) of the annual CO_2 flux. Long-term analysis suggests that antecedent seasonal conditions
684 explained the 64 % efflux that occurred in the spring after ice-off (Finlay et al. 2019). The
685 paucity of published year-round rates makes it difficult to conclude whether most lakes are net
686 autotrophic or heterotrophic. When measured, winter metabolism is an important component of
687 annual O_2 and CO_2 lake budgets, but winter gas releases to the atmosphere tend to be stochastic
688 and brief (Ducharme-Riel et al. 2015) and would not be captured in typical monthly monitoring
689 programs.
690 *Methodological caveats*

691 Comparison of the 3 different methods used to measure AGP and the 2 approaches
692 utilized to estimate AR rates revealed some significant differences, which captures the spatial
693 and temporal integration features and assumptions made with different approaches (Table 3).
694 Incorporating multiple approaches and assumptions is the strength of our message. Each method
695 represents different integration periods, with assumptions of equivalent respiration rates under
696 light and dark conditions (e.g., LD method). We also made comparisons, regardless of the
697 aquatic organisms present, differences in physical factors (i.e., wind) and water column mixing,
698 and inherent assumptions of each technique including conversion factors. The Water-PAM
699 fluorometer measures PSII quantum efficiency and is useful in estimating gross primary
700 production but not respiration. RLCs represent phytoplankton response in minutes, while LD
701 incubations were hours. The $\delta^{18}O$ and LD approaches account for all changes in O_2, which could
702 be attributed to heterotrophic bacterioplankton, zooplankton <200 μm, as well as phytoplankton
703 (which includes prokaryotic cyanobacteria). The conversion factors between the various
704 definitions of GPP (e.g., electron transport as measured by variable fluorescence versus gross O_2
705 evolution) and the variety of assumptions inherent to each technique (e.g., artifacts of non-
706 phytoplankton respiration) also contribute to the methodological differences. Additional studies
707 conducted during the open-water season have method production ratios of 0.66 ($\delta^{18}O$:LD;
708 Ostrom et al. 2005) and 0.84 ($\delta^{18}O$:LD; Bocaniov et al. 2012), compared to our ratio of 1.08 for
709 Lake Simcoe (Table 3). Method comparison respiration ratios, which are very rare in the
710 literature, of 1.35 ($\delta^{18}O$:LD; Bocaniov et al. 2012) are also lower than our reported ratio of 2.87
711 on Lake Simcoe (Table 3). The AR ratio ($\delta^{18}O$:free-water) on Blackstrap was more in line with
712 the LD comparison, while Diefenbaker had a substantially lower ratio (Supplemental
713 Information).

What are the environmental drivers of under-ice production and respiration rates?

As found here, nutrient deficiency is uncommon during the winter and shoulder seasons (Davies et al. 2004; Twiss et al. 2012) and light is most often the limiting factor to phytoplankton (Dokulil et al. 2014; Hampton et al. 2017; Pernica et al. 2017). During the open-water season, both Lakes Simcoe and Diefenbaker are P deficient (Guildford et al. 2013; Dubourg et al. 2015), and dissolved nutrient concentrations are much lower than under-ice (Table 1). We do not expect, therefore, that the under-ice phytoplankton community is nutrient limited. This is also supported by the significant positive relationship between $\bar{E}_{24}$ and AGP_F, indicating light is the primary driver of winter primary production.

Under-ice, primary production typically occurs at the surface of the water column (Yoshida et al., 2003); both phytoplankton biomass (Lenard 2015) and production (Dokulil et al. 2014) can be limited by light and respond quickly to improved light conditions (Hrycik and Stockwell 2020). The under-ice light environment (estimated by $\bar{E}_{24}$) is dictated by convective mixing dynamics (Yang et al. 2020), where convective cells maintain the phytoplankton at the top of the water column (Bertilsson et al. 2013), improving the $\bar{E}_{24}$ (Pernica et al. 2017; Bouffard et al. 2019), resulting in increased phytoplankton biomass (Suarez et al. 2019). This is now a well-documented phenomenon on Lake Simcoe (Pernica et al. 2017), related to winter phytoplankton peaks (Baranowska et al. 2013; Yang et al. 2017). Our companion studies on Lake Simcoe documented these under-ice phytoplankton blooms that were 10 m thick (Pernica et al. 2017) and composed of small centric diatoms (e.g., *Stephanodiscus*), representing 3x more biomass in a single event than measured during the summer sampling (Kim et al. 2015). Late winter phytoplankton peaks related to improved light conditions have also been reported in Placid Lake, Montana, US (Baehr and DeGrandpre 2004). The difference between open-water

737 and under-ice $\bar{E}_{24}$ were only significant on Lakes Diefenbaker and Simcoe in our dataset. In 6
738 European shallow lakes, winter Secchi depths were similar, if not greater, than summer depths
739 (Dokulil et al. 2014). Only 29 % of our under-ice samples indicated light deficiency, and Lake
740 Simcoe demonstrated improved light conditions just prior to ice-off, which resulted in a Chl *a*
741 peak and maximum AGP rates. Similar late winter/early spring under-ice phytoplankton peaks
742 have also been observed on another Saskatchewan reservoir (Cavaliere and Baulch 2020) and
743 Lake Baikal, Russia (Katz et al. 2015). In Lake Sunapee, US, increases in productivity are
744 implied by the O_2 increase at the end of winter and subsequent shift to autotrophy (Brentrup et al.
745 2021). The length of winter was found to be an important factor in this shift, where ice-on and
746 ice-off periods were drivers of annual metabolism estimates (Brentrup et al. 2021).
747 Phytoplankton response to light can be assessed with P-E parameters that quantitatively
748 describe aspects of phytoplankton photophysiology. Fluorescence-based measurements have
749 previously been used to assess photosynthetic potential of winter phytoplankton in Lake Erie
750 (Twiss et al. 2012; Edgar et al. 2016) and in ice-covered reservoirs in the Czech Republic
751 (McKay et al. 2015). Consistent with our results, these studies found that winter phytoplankton
752 are photosynthetically active and physiologically robust (Twiss et al. 2012; McKay et al. 2015;
753 Edgar et al. 2016). The light saturation parameter, E_k, is an indicator of the phytoplankton
754 community's photoacclimation status. If the ratio of $\bar{E}_{24}/E_k$ is less than one, light deficient
755 conditions are expected. This was the case for 3 of our water bodies under ice cover, with the
756 fourth (Lake Simcoe) showing an $\bar{E}_{24}/E_k$ ratio of 1.4 (Table 1). During the winter, phytoplankton
757 acclimate to low-light conditions, as evidenced by low E_k values on Lake Balaton (55.9 µmol m^{-2}
758 s^{-1}) and Neusiedler See (30 µmol m^{-2} s^{-1}; Dokulil et al. 2014); considerably lower than our winter
759 E_k values which ranged from 78.7–354.2 µmol m^{-2} s^{-1} (Table 1). In ice-covered Lake Erie, E_k

760 was lower still (~10 µmol m^{-2} s^{-1}; Edgar et al. 2016). Winter-to-summer comparisons on Lake
761 Balaton and Neusiedler See demonstrated that E_k was 6x lower in the winter (Dokulil et al.
762 2014), while in our dataset, E_k was only 2x lower in the winter. In these European lakes, P_{max} was
763 6x lower in winter than summer (Dokulil et al. 2014), while in our data set, $rETR_{max}$ was only 4x
764 lower in winter (Table 1). Under-ice phytoplankton populations in our study ecosystems have
765 adjusted to the low light environment by photoacclimating, which is reflected by the lack of
766 relationship between POC and Chl *a* concentrations. Our demonstration that Chl *a* does not
767 represent phytoplankton biomass in the winter is supported by other studies that showed
768 discrepancies between phytoplankton biomass and Chl *a* concentrations in under-ice samples
769 (Lenard 2015). Photoacclimation has implications for broader applications such as winter
770 limnology studies where Chl *a* is assumed to represent under-ice algal biomass (Hampton et al.
771 2017).

772 *Implications for lake management*

773 An inherent assumption in lake management is that primary production is positively
774 related to phytoplankton biomass. A disconnect, however, between production and biomass has
775 been observed in relatively turbid water bodies (Dubourg et al. 2015; Petty et al. 2020). In our
776 similarly winter light deficient conditions, 50 % of the time under-ice PAR was deficient for
777 biomass accrual in our Canadian water bodies, although in Lake Erie, winter phytoplankton
778 growth rates were comparable to summer (Twiss et al. 2014). It is unclear if the recent reporting
779 of under-ice blooms (Öterler 2017; Ewing et al. 2020; Wen et al. 2020) will translate to increases
780 in primary production with perceived shifts to autotrophic conditions during the winter season.
781 Certainly, the increase in motile phytoplankton, including potentially toxin-producing

782 cyanobacteria (e.g., *Planktothrix rubescens*; Dokulil and Herzig 2009; Lenard 2015b), which
783 exhibit metalimnetic peaks, has implications for human health and lake management.
784 *What can we expect in a warmer and ice-free future?*
785 Overlaid on the climate-induced reductions in ice cover (Sharma et al. 2019), climate
786 predictions also suggest that there will be less snow cover (both depth and duration; DeBeer et
787 al. 2016). Ice and snow removal experiments provide some insights into what this means for
788 future lake metabolism and the role that temperate lakes play in global carbon and O_2 budgets. In
789 an experimental study when 50 % of the ice cover was removed, a significant decrease in GPP
790 occurred (Hamdan et al. 2018), likely related to changes in convective mixing and the resultant
791 light environment. The importance of snow on under-ice metabolism has been established
792 (Obertegger et al. 2017); experimental snow removal resulted in an increase in AGP (Garcia et
793 al. 2019). Increased production will result in increased O_2 concentrations, which may prevent
794 winter fish kills. An increase in phytoplankton lipids will also support winter zooplankton
795 populations (Grosbois et al. 2017; Hrycik et al. 2017), which will support fish and increase
796 aquatic biodiversity (Hrycik et al. 2017; McMeans et al. 2017). Temporal changes in
797 phytoplankton peaks as a result of changing winters could also cause potential shifts in lake
798 ecology. For example, a temporal mismatch between algal peaks and zooplankton egg hatching
799 could result in cascading effects in food webs. The alternative stable state hypothesis posits that
800 ecosystems maintain resilience and do not experience state change until a disturbance shifts the
801 ecosystem (Scheffer et al. 1993). Climate change will shift the physical functioning of water
802 bodies, modifying the doctrine of phytoplankton community seasonality (Wetzel 2001). Due to
803 their unique attributes, competition theory indicates that cyanobacteria will have the advantage
804 over eukaryotic phytoplankton in these alternative stable states (Brauer et al. 2012).

Here, we advance our understanding of winter limnology under a changing climate. Once we recognize the importance of the winter and shoulder seasons and the implications of changing seasonal dynamics, we can make the leap to develop new hypotheses. Transient peaks in biomass and production matter, and should be considered in predictive lake models. The current lack of year-round data is a major impediment to predict the effect of a changing climate on lake ecology and biogeochemistry.

References

Adrian, R., R. Deneke, U. Mischke, R. Stellmacher, and P. Lederer. 1995. A long-term study of the Heliligensee (1975-1992). Evidence for effects of climate change on the dynamics of eutrophied lake ecosystems. Arch. Fur Hydrobiol. **133**: 315–337.

Adrian, R., N. Walz, T. Hintze, S. Hoeg, and R. Rusche. 1999. Effects of ice duration on plankton succession during spring in a shallow polymictic lake. Freshw. Biol. **41**: 621–632. doi:10.1046/j.1365-2427.1999.00411.x

Arrigo, K. R., M. M. Mills, L. R. Kropuenske, G. L. Van Dijken, A. C. Alderkamp, and D. H. Robinson. 2010. Photophysiology in two major southern ocean phytoplankton taxa: Photosynthesis and growth of phaeocystis antarctica and fragilariopsis cylindrus under different irradiance levels. Integr. Comp. Biol. **50**: 950–966. doi:10.1093/icb/icq021

Bachmann, R. W., and D. E. Canfield. 1996. Use of an alternative method for monitoring total nitrogen concentrations in Florida lakes. Hydrobiologia **323**: 1–8.

Baehr, M. M., and M. D. DeGrandpre. 2004. In situ pCO(2) and O-2 measurements in a lake during turnover and stratification: Observations and modeling. Limnol. Oceanogr. **49**: 330–340.

Baranowska, K. A., R. L. North, J. G. Winter, and P. J. Dillon. 2013. Long-term seasonal effects of dreissenid mussels on phytoplankton in Lake Simcoe, Ontario, Canada. Inl. Waters **3**: 285–296. doi:10.5268/IW-3.2.527

Bashenkhaeva, M. V., Y. R. Zakharova, D. P. Petrova, I. V. Khanaev, Y. P. Galachyants, and Y. V. Likhoshway. 2015. Sub-ice microalgal and bacterial communities in freshwater Lake

832 Baikal, Russia. Microb. Ecol. **70**: 751–765. doi:10.1007/s00248-015-0619-2

833 Belzile, C., W. F. Vincent, J. A. E. Gibson, and P. Van Hove. 2001. Bio-optical characteristics of
834 the snow, ice, and water column of a perennially ice-covered lake in the High Arctic. Can.
835 J. Fish. Aquat. Sci. **58**: 2405–2418. doi:10.1139/cjfas-58-12-2405

836 Benson, B., and D. J. Krause. 1984. The concentration and isotopic fractionation of oxygen
837 dissolved in freshwater and seawater in equilibrium with the atmosphere. Limnol. Ocean.
838 **29**: 620–632.

839 Benson, B., D. J. Krause, and M. Peterson. 1979. The solubility and isotopic fractionation of
840 gases in dilute aquatic solution I. Oxygen. J Solut. Chem **8**: 655–690.

841 Bergmann, M., and R. H. Peters. 1980. A simple reflectance method for the measurement of
842 particulate pigment in lake water and its application to phosphorus-chlorophyll-seston
843 relationship. Can. J. Fish. Aquat. Sci. **3**: 111–114. doi:10.1139/f80-011

844 Bertilsson, S., A. Burgin, C. C. Carey, and others. 2013. The under-ice microbiome of seasonally
845 frozen lakes. Limnol. Oceanogr. **58**: 1998–2012. doi:10.4319/lo.2013.58.6.1998

846 Biddanda, B. A., and J. B. Cotner. 2002. Love handles in aquatic ecosystems: The role of
847 dissolved organic carbon drawdown, resuspended sediments, and terrigenous inputs in the
848 carbon balance of Lake Michigan. Ecosystems **5**: 431–445.

849 Block, B. D., B. A. Denfeld, J. D. Stockwell, and others. 2019. The unique methodological
850 challenges of winter limnology. Limnol. Oceanogr. Methods **17**: 42–57.
851 doi:10.1002/lom3.10295

852 Bocaniov, S. A., S. L. Schiff, and R. E. H. Smith. 2012. Plankton metabolism and physical

853 forcing in a productive embayment of a large oligotrophic lake: insights from stable oxygen
854 isotopes. Freshw. Biol. **57**: 481–496. doi:10.1111/j.1365-2427.2011.02715.x

855 Bocaniov, S. A., S. L. Schiff, and R. E. H. Smith. 2015. Non steady-state dynamics of stable
856 oxygen isotopes for estimates of metabolic balance in large lakes. J. Great Lakes Res. **41**:
857 719–729. doi:10.1016/j.jglr.2015.05.013

858 Bocaniov, S. A., and R. E. H. Smith. 2009. Plankton metabolic balance at the margins of very
859 large lakes: temporal variability and evidence for dominance of autochthonous processes.
860 Freshw. Biol. **54**: 345–362. doi:doi: 10.1111/j.1365-2427.2008.02120.x

861 Bouffard, D., G. Zdorovennova, S. Bogdanov, and others. 2019. Under-ice convection dynamics
862 in a boreal lake. Inl. Waters **9**: 142–161. doi:10.1080/20442041.2018.1533356

863 Brauer, V. S., M. Stomp, and J. Huisman. 2012. The nutrient-load hypothesis: patterns of
864 resource limitation and community structure driven by competition for nutrients and light.
865 Am. Nat. **179**: 721–740. doi:10.1086/665650

866 Brentrup, J. A., D. C. Richardson, C. C. Carey, and others. 2021. Under-ice respiration rates shift
867 the annual carbon cycle in the mixed layer of an oligotrophic lake from autotrophy to
868 heterotrophy. Inl. Waters **11**: 114–123. doi:10.1080/20442041.2020.1805261

869 Butts, E., and H. J. Carrick. 2017. Phytoplankton seasonality along a trophic gradient of
870 temperate lakes: Convergence in taxonomic compostion during winter ice-cover. Northeast.
871 Nat. **24**: B167–B187. doi:10.1656/045.024.s719

872 Camurri, I., I. Ferrari, and M. Villani. 1976. Biomassa e produczione del fitoplancton nel lago
873 Santo Parmense nella stagione delle acque aperte. Arch. Ocean. Limnol. **18**: 237–253.

874 Carignan, R., A. M. Blais, and C. Vis. 1998. Measurement of primary production and
875 community respiration in oligotrophic lakes using the Winkler method. Can. J. Fish. Aquat.
876 Sci. **55**: 1078–1084.

877 Cavaliere, E., and H. M. Baulch. 2018. Denitrification under lake ice. Biogeochemistry **137**:
878 285–295. doi:10.1007/s10533-018-0419-0

879 Cavaliere, E., and H. M. Baulch. 2020. Winter in two phases: Long-term study of a shallow
880 reservoir in winter. Limnol. Oceanogr. 1–18. doi:10.1002/lno.11687

881 Chorus, I., and E. Spijkerman. 2021. What Colin Reynolds could tell us about nutrient limitation,
882 N : P ratios and eutrophication control. Hydrobiologia **848**: 95–111. doi:10.1007/s10750-
883 020-04377-w

884 Cole, J. I., and N. Caraco. 1998. Atmospheric exchange of carbon dioxide in a low-wind
885 oligotrophic lake measured by the addition of SF6. Limnol. Ocean. **43**: 647–656.

886 Crumpton, W., T. Isenhart, and P. Mitchell. 1992. Nitrate and organic N analyses with second-
887 derivative spectroscopy. Limnol. Oceanogr. **37**: 907–913.

888 Crusius, J., and R. Wanninkhof. 2003. Gas transfer velocities measured at low wind speed over a
889 lake. Limnol. Ocean. **48**: 1010–1017.

890 D'souza, N. A. 2012. Psychrophilic diatoms in ice-covered Lake Erie. Bowling Green State
891 University.

892 Davies, J.-M., W. H. Nowlin, and A. Mazumder. 2004. Temporal changes in nitrogen and
893 phosphorus codeficiency of plankton in lakes of coastal and interior British Columbia. Can.
894 J. Fish. Aquat. Sci. **61**: 1538–1551. doi:10.1139/f04-092

DeBeer, C. M., H. S. Wheater, S. K. Carey, and K. P. Chun. 2016. Recent climatic, cryospheric, and hydrological changes over the interior of western Canada: A review and synthesis. Hydrol. Earth Syst. Sci. **20**: 1573–1598. doi:10.5194/hess-20-1573-2016

Denfeld, B. A., H. M. Baulch, P. A. del Giorgio, S. E. Hampton, and J. Karlsson. 2018. A synthesis of carbon dioxide and methane dynamics during the ice-covered period of northern lakes. Limnol. Oceanogr. Lett. **3**: 117–131. doi:10.1002/lol2.10079

Depew, D. C., S. J. Guildford, and R. E. H. Smith. 2006a. Nearshore – offshore comparison of chlorophyll a and phytoplankton production in the dreissenid- colonized eastern basin of Lake Erie. Can. J. Fish. Aquat. Sci. **63**: 1115–1129. doi:10.1139/F06-016

Depew, D., R. Smith, and S. Guildford. 2006b. Production and respiration in Lake Erie plankton communities. J. Gt. Lakes Res. **32**: 817–831.

Dokulil, M. T., and A. Herzig. 2009. An analysis of long-term winter data on phytoplankton and zooplankton in Neusiedler See, a shallow temperate lake, Austria. Aquat. Ecol. **43**: 715–725. doi:10.1007/s10452-009-9282-3

Dokulil, M. T., A. Herzig, B. Somogyi, L. Vörös, K. Donabaum, L. May, and T. Nõges. 2014. Winter conditions in six European shallow lakes: A comparative synopsis. Est. J. Ecol. **63**: 111–129. doi:10.3176/eco.2014.3.01

Dubourg, P., R. L. North, K. Hunter, D. M. Vandergucht, O. Abirhire, G. M. Silsbe, S. J. Guildford, and J. J. Hudson. 2015. Light and nutrient co-limitation of phytoplankton communities in a large reservoir: Lake Diefenbaker, Saskatchewan, Canada. J. Great Lakes Res. **41**: 129–143. doi:10.1016/j.jglr.2015.10.001

916 Ducharme-Riel, V., D. Vachon, P. A. del Giorgio, and Y. T. Prairie. 2015. The relative
917 contribution of winter under-ice and summer hypolimnetic CO2 accumulation to the annual
918 CO2 emissions from northern lakes. Ecosystems **18**: 547–559. doi:10.1007/s10021-015-
919 9846-0

920 Edgar, R. E., P. F. Morris, M. J. Rozmarynowycz, and others. 2016. Adaptations to
921 photoautotrophy associated with seasonal ice cover in a large lake revealed by
922 metatranscriptome analysis of a winter diatom bloom. J. Great Lakes Res.
923 doi:10.1016/j.jglr.2016.07.025

924 Ewing, H., K. C. Weathers, K. L. Cottingham, and others. 2020. " New " cyanobacterial blooms
925 are not new : two centuries of lake production are related to ice cover and land use.
926 Ecosphere **11**. doi:10.1002/ecs2.3170

927 Ferrari, I. 1976. Winter limnology of a mountain lake - Lago Santo-Parmense (Northern
928 Appennines, Italy). Hydrobiologia **51**: 245–257.

929 Findlay, D. L., and H. J. Kling. 1998. Protocols for measuring biodiversity: Phytoplankton in
930 freshwater.

931 Finlay, K., R. J. Vogt, G. L. Simpson, and P. R. Leavitt. 2019. Seasonality of pCO 2 in a hard-
932 water lake of the northern Great Plains: The legacy effects of climate and limnological
933 conditions over 36 years. Limnol. Oceanogr. **64**: S118–S129. doi:10.1002/lno.11113

934 Gammons, C. H., W. Henne, S. R. Poulson, S. R. Parker, T. B. Johnston, J. E. Dore, and E. S.
935 Boyd. 2014. Stable isotopes track biogeochemical processes under seasonal ice cover in a
936 shallow, productive lake. Biogeochemistry **120**: 359–379. doi:10.1007/s10533-014-0005-z

Gammons, C. H., B. L. Pape, S. R. Parker, S. R. Poulson, and C. E. Blank. 2013. Geochemistry, water balance, and stable isotopes of a “clean” pit lake at an abandoned tungsten mine, Montana, USA. Appl. Geochemistry **36**: 57–69. doi:10.1016/j.apgeochem.2013.06.011

Garcia, S. L., A. J. Szekely, C. Bergvall, M. Schattenhofer, and S. Peura. 2019. Decreased snow cover stimulates under-ice primary producers but impairs methanotrophic capacity. mSphere **4**. doi:10.1128/msphere.00626-18

Del Giorgio, P. a., and R. H. Peters. 1994. Patterns in planktonic P:R ratios in lakes: Influence of lake trophy and dissolved organic carbon. Limnol. Oceanogr. **39**: 772–787. doi:10.4319/lo.1994.39.4.0772

Glooschenko, W. A., J. E. Moore, M. Munawar, and R. A. Vollenweider. 1974. Primary production in Lakes Ontario and Erie: A comparative study. J. Fish. Res. Board Can. **31**: 253–263.

Gosselin, M., L. Legendre, S. Demers, and R. G. Ingram. 1985. Responses of sea-ice microalgae to climatic and fortnightly tidal energy imputs. (Mannitouk Sound, Hudson Bay). Can. J. Fish. Aquat. Sci. **42**: 999–1006. doi:10.1139/f85-125

Grosbois, G., H. Mariash, T. Schneider, and M. Rautio. 2017. Under-ice availability of phytoplankton lipids is key to freshwater zooplankton winter survival. Sci. Rep. **7**: 1–11. doi:10.1038/s41598-017-10956-0

Grosbois, G., D. Vachon, P. A. del Giorgio, and M. Rautio. 2020. Efficiency of crustacean zooplankton in transferring allochthonous carbon in a boreal lake. Ecology **101**. doi:10.1002/ecy.3013

Guildford, S. J., D. C. Depew, T. Ozersky, R. E. Hecky, and R. E. H. Smith. 2013. Nearshore-offshore differences in planktonic chlorophyll and phytoplankton nutrient status after dreissenid establishment in a large shallow lake. Inl. Waters **3**: 253–268. doi:10.5268/iw-3.2.537

Guy, R., J. Berry, M. Fogel, and T. Hoering. 1989. Differential fractionation of oxygen isotopes by cyanide-resistant and cyanide-sensitive respiration in plants. Planta **177**: 483–491.

Guy, R., M. Fogel, and J. Berry. 1993. Photosynthetic fractionation of the stable isotopes of oxygen and carbon. Plant Physiol **101**: 37–47.

Hamdan, M., P. Byström, E. R. Hotchkiss, M. J. Al-Haidarey, J. Ask, and J. Karlsson. 2018. Carbon dioxide stimulates lake primary production. Sci. Rep. **8**: 8–12. doi:10.1038/s41598-018-29166-3

Hampton, S. E., A. W. E. Galloway, S. M. Powers, and others. 2017. Ecology under lake ice. Ecol. Lett. **20**: 98–111. doi:10.1111/ele.12699

Hampton, S. E., D. K. Gray, L. R. Izmest'eva, M. V. Moore, and T. Ozersky. 2014. The rise and fall of plankton: Long-term changes in the vertical distribution of algae and grazers in Lake Baikal, Siberia. PLoS One **9**: 1–10. doi:10.1371/journal.pone.0088920

Hampton, S. E., M. V Moore, T. Ozersky, E. H. Stanley, C. M. Polashenski, and A. W. E. Galloway. 2015. Heating up a cold subject: prospects for under-ice plankton research in lakes. J. Plankton Res. **37**: 277–284. doi:10.1093/plankt/fbv002

Hanson, P. C., D. L. Bade, S. R. Carpenter, and T. K. Kratz. 2003. Lake metabolism: Relationships with dissolved organic carbon and phosphorus. Limnol. Oceanogr. **48**: 1112–

1119. doi:10.4319/lo.2003.48.3.1112

Hecky, R. E., and S. J. Guildford. 1984. Primary productivity of Southern Indian Lake before, during, and after impoundment and Churchill River diversion. Can. J. Fish. Aquat. Sci. **41**: 591–604.

Helman, Y., E. Barkan, D. Eisenstadt, B. Luz, and A. Kaplan. 2005. Fractionation of the three stable oxygen isotopes by oxygen-producing and oxygen-consuming reactions in photosynthetic organisms. Plant Physiol **138**: 2292–2298.

Henshaw, T., and J. Laybourn-Parry. 2002. The annual patterns of photosynthesis in two large, freshwater, ultra-oligotrophic Antarctic lakes. Polar Biol. **25**: 744–752. doi:10.1007/s00300-002-0402-y

Holmes, R. M., A. Aminot, R. Kerouel, B. A. Hooker, and B. J. Peterson. 1999. A simple and precise method for measuring ammonium in marine and freshwater ecosystems. Can. J. Fish. Aquat. Sci. **56**: 1801–1808. doi:10.1139/cjfas-56-10-1801

Hrycik, A. R., and J. D. Stockwell. 2020. Under-ice mesocosms reveal the primacy of light but the importance of zooplankton in winter phytoplankton dynamics. Limnol. Oceanogr. 1–15. doi:10.1002/lno.11618

Hrycik, A. R., J. D. Stockwell, J. S. Rabaey, and others. 2017. Winter in water: differential responses and the maintenance of biodiversity. Inl. Waters **9**: 715–725. doi:10.1016/j.ejrh.2021.100780

Idrizaj, A., A. Laas, U. Anijalg, and P. Nõges. 2016. Horizontal differences in ecosystem metabolism of a large shallow lake. J. Hydrol. **535**: 93–100.

doi:10.1016/j.jhydrol.2016.01.037

Jähne, B., K. O. Münnich, R. Bösinger, A. Dutzi, W. Huber, and P. Libner. 1987. On the parameters influencing air-water gas exchange. J. Geophys. Res. **92**: 1937–1949.

Kalff, J., and H. E. Welch. 1974. Phytoplankton production in Char Lake, a natural polar lake, and in Meretta Lake, a polluted polar lake, Cornwallis-Island, Northwest-Territories. J. Fish. Res. Board Canada **31**: 621–636.

Kalinowska, K., and M. Grabowska. 2016. Autotrophic and heterotrophic plankton under ice in a eutrophic temperate lake. Hydrobiologia **777**: 111–118. doi:10.1007/s10750-016-2769-8

Katz, S. L., L. R. Izmest'eva, S. E. Hampton, T. Ozersky, K. Shchapov, M. V Moore, S. V Shimaraeva, and E. A. Silow. 2015. The "Melosira years" of Lake Baikal: Winter environmental conditions at ice onset predict under-ice algal blooms in spring. Limnol. Oceanogr. **60**: 1950–1964. doi:10.1002/lno.10143

Kiddon, J., M. Bender, J. Orchardo, D. Caron, J. Goldman, and M. Dennett. 1993. Isotopic fractionation of oxygen by respiring marine organisms. Glob. Biogeochem Cycles **7**: 679–694.

Kim, T. Y., R. L. North, S. J. Guildford, P. Dillon, and R. E. H. Smith. 2015. Phytoplankton productivity and size composition in Lake Simcoe: The nearshore shunt and the importance of autumnal production. J. Great Lakes Res. **41**: 1075–1086. doi:10.1016/j.jglr.2015.09.011

Kirk, J. T. O. 1994. Light and photosynthesis in aquatic ecosystems, Oxford University Press.

Knox, M., P. Quay, and D. Wilbur. 1992. Kinetic isotopic fractionation during air–water gas transfer of O2 , N2 , CH4 , and H2. J Geophys Res **97**: 20335–20343.

1021 Kroopnick, P., and H. Craig. 1972. Atmospheric oxygen: Isotopic composition and solubility
1022 fractionation. Science (80-.). **175**: 54–55.

1023 Lenard, T. 2015. Winter bloom of some motile phytoplankton under ice cover in a mesotrophic
1024 lake: vertical distribution and environmental factors. Oceanol. Hydrobiol. Stud. **44**: 164–
1025 171. doi:10.1515/ohs-2015-0016

1026 Livingstone, D. M., and R. Adrian. 2009. Modeling the duration of intermittent ice cover on a
1027 lake for climate-change studies. Limnol. Oceanogr. **54**: 1709–1722.

1028 Maeda, O., and S. Ichimura. 1973. On the high density of a phytoplankton population found in a
1029 lake under ice. Int. Rev. der gesamten Hydrobiol. **5**: 673–689.

1030 Magnuson, J. J., D. M. Robertson, B. J. Benson, and others. 2000. Historical trends in lake and
1031 river ice cover in the northern hemisphere. Science (80-.). **289**: 1743–1746.
1032 doi:10.1126/science.289.5485.1743

1033 McKay, R. M. L., O. Prášil, L. Pechar, E. Lawrenz, M. J. Rozmarynowycz, and G. S. Bullerjahn.
1034 2015. Freshwater ice as habitat: Partitioning of phytoplankton and bacteria between ice and
1035 water in central European reservoirs. Environ. Microbiol. Rep. **7**: 887–898.
1036 doi:10.1111/1758-2229.12322

1037 McMeans, B. C., K. S. McCann, M. M. Guzzo, and others. 2017. High-frequency observations
1038 of temperature and dissolved oxygen reveal under-ice convection in a large lake. Inl. Waters
1039 **9**: 12,218-12,226. doi:10.1002/2017GL075373

1040 McMeans, B. C., K. S. McCann, M. M. Guzzo, and others. 2020. Winter in water: differential
1041 responses and the maintenance of biodiversity. Ecol. Lett. **23**: 922–938.

doi:10.1111/ele.13504

Noges, T., and P. Noges. 1999. The effect of extreme water level decrease on hydrochemistry and phytoplankton in a shallow eutrophic lake. Hydrobiologia **408**: 277–283.

North, R. L., D. Barton, A. S. Crowe, and others. 2013. The state of Lake Simcoe (Ontario, Canada): The effects of multiple stressors on phosphorus and oxygen dynamics. Inl. Waters **3**: 51–74. doi:10.5268/IW-3.1.529

North, R. L., J. Johansson, D. M. Vandergucht, L. E. Doig, K. Liber, K. E. Lindenschmidt, H. Baulch, and J. J. Hudson. 2015. Evidence for internal phosphorus loading in a large prairie reservoir (Lake Diefenbaker, Saskatchewan). J. Great Lakes Res. doi:10.1016/j.jglr.2015.07.003

North, R.L., J.J. Venkiteswaran, G. Silsbe, J.W. Harrison, J.J. Hudson, R.E. Smith, P.J. Dillon, P.J. Pernica, S.J. Guildford, M. Kehoe, and H.M. Baulch. 2023. Year-round metabolism data from Lakes Simcoe (Ontario, 2010-2011), Diefenbaker, Blackstrap, and Broderick (Saskatchewan, 2013-2014), Canada. ver 2. Environmental Data Initiative. https://doi.org/10.6073/pasta/ac92e6eb81acf4b3d6701aa296550dc2 (Accessed 2023-01-30).

NSIDC: National Snow and Ice Data Center. 2008. U.S. National Ice Center. IMS Dly. North. Hemisph. Snow Ice Anal. 1 km, 4 km, 24 km Resolut. Version 1. Boulder, Color. USA. doi:https://doi.org/10.7265/N52R3PMC

Obertegger, U., B. Obrador, and G. Flaim. 2017. Dissolved oxygen dynamics under ice : three winters of high frequency data from Lake Tovel, Italy. Water Resour. Res. **53**: 7234–7246.

Ontario Ministry of the Environment (OMOE). 2007a. The determination of total phosphorus in

1063 water by colourimetry.

1064 Ontario Ministry of the Environment (OMOE). 2007b. The determination of ammonia nitrogen
1065 and nitrate plus nitritie nitrogen in water and precipitation by colourimetry.

1066 Ontario Ministry of the Environment (OMOE). 2008. The determination of total kjeldahl
1067 nitrogen in surface water and precipitation by colourimetry.

1068 Ostrom, N. E., H. J. Carrick, M. R. Twiss, and L. Piwinski. 2005. Evaluation of primary
1069 production in Lake Erie by multiple proxies. Oecologia **144**: 115–124. doi:DOI:
1070 10.1007/s00442-005-0032-5

1071 Öterler, B. 2017. Winter phytoplankton composition occurring in a temporarily ice-covered lake:
1072 A case study. Polish J. Environ. Stud. **26**: 2677–2688. doi:10.15244/pjoes/74015

1073 Ozersky, T., A. Bramburger, A. Elgin, and others. 2021. The changing face of winter: Lessons
1074 and questions from the Laurentian Great Lakes. J. Geophys. Res. Biogeosciences **126**:
1075 e2021JG006247.

1076 Parsons, T. R., Y. Maita, and C. M. Lalli. 1984. A manual of chemical and biological methods
1077 for seawater analysis, Pergamon.

1078 Pernica, P., R. L. North, and H. M. Baulch. 2017. In the cold light of day : the potential
1079 importance of under-ice convective mixed layers to primary producers. Inl. Waters **7**: 138–
1080 150. doi:10.1080/20442041.2017.1296627

1081 Petty, E. L., D. V. Obrecht, and R. L. North. 2020. Filling in the flyover zone: high phosphorus
1082 in Midwestern (USA) reservoirs results in high phytoplankton biomass but not high primary
1083 productivity. Front. Environ. Sci. **8**.

Powers, S. M., H. M. Baulch, S. E. Hampton, S. G. Labou, N. R. Lottig, and E. H. Stanley. 2017a. Nitrification contributes to winter oxygen depletion in seasonally frozen forested lakes. Biogeochemistry **136**: 119–129. doi:10.1007/s10533-017-0382-1

Powers, S. M., S. G. Labou, H. M. Baulch, R. J. Hunt, N. R. Lottig, S. E. Hampton, and E. H. Stanley. 2017b. Ice duration drives winter nitrate accumulation in north temperate lakes. Limnol. Oceanogr. Lett. **2**: 177–186. doi:10.1002/lol2.10048

Quay, P. D., D. O. Wilbur, J. E. Richey, A. H. Devol, R. Benner, and B. R. Forsberg. 1995. The ^{18}O:^{16}O of dissolved oxygen in rivers and lakes in the Amazon Basin: Determining the ratio of respiration to photosynthesis rates in freshwaters. Limnol. Oceanogr. **40**: 718–729. doi:10.4319/lo.1995.40.4.0718

Quinn, C. J., R. L. North, and P. J. Dillon. 2013. Year-round patterns in bacterial production and biomass in Lake Simcoe, Ontario, Canada: are heterotrophic bacteria a significant contributor to low hypolimnetic oxygen? Inl. Waters **3**: 235–252. doi:10.5268/iw-3.2.536

Rabaey, J. S., L. M. Domine, K. D. Zimmer, and J. B. Cotner. 2021. Winter oxygen regimes in clear and turbid shallow lakes. JGR Biogeosciences.

Sadeghian, A., D. de Boer, J. J. Hudson, H. Wheater, and K. E. Lindenschmidt. 2015. Lake Diefenbaker temperature model. J. Great Lakes Res. **41**: 8–21. doi:10.1016/j.jglr.2015.10.002

Saxton, M. A., N. A. D'souza, R. A. Bourbonniere, R. M. L. McKay, and S. W. Wilhelm. 2012. Seasonal Si:C ratios in Lake Erie diatoms - Evidence of an active winter diatom community. J. Great Lakes Res. **38**: 206–211. doi:10.1016/j.jglr.2012.02.009

1105 Scheffer, M., S. H. Hosper, M. L. Meijer, B. Moss, and E. Jeppesen. 1993. Alternative equilibria
1106 in shallow lakes. Trends Ecol. Evol. **8**: 275–279. doi:10.1016/0169-5347(93)90254-m

1107 Sharma, S., K. Blagrave, J. J. Magnuson, and others. 2019. Widespread loss of lake ice around
1108 the Northern Hemisphere in a warming world. Nat. Clim. Chang. **9**: 227–231.
1109 doi:10.1038/s41558-018-0393-5

1110 Silsbe, G. M., R. E. Hecky, and R. E. H. Smith. 2012. Improved estimation of carbon fixation
1111 rates from active flourometry using spectral fluorescence in light-limited environments.
1112 Limnol. Oceanogr. Methods **10**: 736–751. doi:10.4319/lom.2012.10.736

1113 Silsbe, G. M., and J. C. Kromkamp. 2012. Modeling the irradiance dependency of the quantum
1114 efficiency of photosynthesis. Limnol. Oceanogr. Methods **10**: 645–652.
1115 doi:10.4319/lom.2012.10.645

1116 Silsbe, G. M., and S. Y. Malkin. 2015. phytotools: Phytoplankton Production Tools.

1117 Smith, R. E. H., V. P. Hiriart-Baer, S. N. Higgins, S. J. Guildford, and M. N. Charlton. 2005.
1118 Planktonic primary production in the offshore waters of dreissenid-infested Lake Erie in
1119 1997. J. Gt. Lakes Res. **31**: 50–62.

1120 Soetaert, K., T. Petzoldt, and R. W. Setzer. 2010. Solving Differential Equations in R: Package
1121 deSolve. J. Stat. Softw. **33**: 1–25.

1122 Solomon, C. T., D. A. Bruesewitz, D. C. Richardson, and others. 2013. Ecosystem respiration:
1123 Drivers of daily variability and background respiration in lakes around the globe. Limnol.
1124 Oceanogr. **58**: 849–866. doi:10.4319/lo.2013.58.3.0849

1125 Stainton, M. P., M. J. Capel, and F. A. J. Armstrong. 1977. The Chemical Analysis of

Freshwater. 2nd ed. Can. Fish. Mar. Serv. Misc. Spec. Publ.,.

Stevens, C., D. Schultz, C. Vanbaalen, and P. Parker. 1975. Oxygen isotope fractionation during photosynthesis in a blue-green and a green-alga. Plant Physiol **56**: 126–129.

Suarez, E. L., M. C. Tiffay, N. Kalinkina, and others. 2019. Diurnal variation in the convection-driven vertical distribution of phytoplankton under ice and after ice-off in large Lake Onego (Russia). Inl. Waters **9**: 193–204. doi:10.1080/20442041.2018.1559582

Tassan, S., and G. M. Ferrari. 1995. An alternative approach to absorption measurements of aquatic particles retained on filters. Limnol. Oceanogr. **40**: 1358–1368.

Twiss, M. R., R. M. L. McKay, R. A. Bourbonniere, and others. 2012. Diatoms abound in ice-covered Lake Erie: An investigation of offshore winter limnology in Lake Erie over the period 2007 to 2010. J. Great Lakes Res. **38**: 18–30. doi:10.1016/j.jglr.2011.12.008

Twiss, M. R., D. E. Smith, E. M. Cafferty, and H. J. Carrick. 2014. Phytoplankton growth dynamics in offshore Lake Erie during mid-winter. J. Great Lakes Res. **40**: 449–454. doi:10.1016/j.jglr.2014.03.010

Wassenaar, L. I. 2012. Dissolved oxygen status of Lake Winnipeg : Spatio-temporal and isotopic (δ 18 O – O 2) patterns. J. Great Lakes Res. **38**: 123–134. doi:10.1016/j.jglr.2010.12.011

Webb, D. J., B. K. Burnison, A. M. Trimbee, and E. E. Prepas. 1992. Comparison of chlorophyll a extractions with ethanol and dimethyl sulfoxide/acetone, and a concern about spectrophotometric phaeopigment correction. Can. J. Fish. Aquat. Sci. **49**: 2331–2336. doi:10.1139/f92-256

Webb, W. L., M. Newton, and D. Starr. 1974. Carbon dioxide exchange of Alnus rubra.

Oecologia **17**: 281–291.

Wen, Z., K. Song, Y. Shang, and others. 2020. Variability of chlorophyll and the influence factors during winter in seasonally ice-covered lakes. J. Environ. Manage. **276**: 111338. doi:10.1016/j.jenvman.2020.111338

Wetzel, R. G. 1966. Productivity and nutrient relationships in marl lakes of northern Indiana. Verh. Int. Ver. Limnol. **16**: 321–332.

Wetzel, R. G. 2001. Limnology: Lake and River Ecosystems.

Yang, B., M. G. Wells, J. Li, and J. Young. 2020. Mixing, stratification, and plankton under lake-ice during winter in a large lake: Implications for spring dissolved oxygen levels. Limnol. Oceanogr. **65**: 2713–2729. doi:10.1002/lno.11543

Yang, B., J. Young, L. Brown, and M. Wells. 2017. High-Frequency Observations of Temperature and Dissolved Oxygen Reveal Under-Ice Convection in a Large Lake. Geophys. Res. Lett. **44**: 12,218-12,226. doi:10.1002/2017GL075373

Yoshida, T., Sekino, T., Genkai-Kato, M., Logacheva, N. P., Bondarenko, N. A., Kawabata, Z., Khodzher, T. V., Melnik, N. G., Hino, S., Nozaki, K., Nishimura, Y., Nagata, T., Higashi, M. and Nakanishi, M. 2003. Seasonal dynamics of primary production in the pelagic zone of southern Lake Baikal. Limnology. **4**: 53–62. doi:10.1007/s10201-002-0089-3.

Acknowledgements

Funding: Environment Canada's Lake Simcoe Clean-up Fund (LSCUF; REHS, PJD), NSERC (HMB, PJD, SLS, JJH: RGPIN-250060-20), CUPE PDF to RLN, Global Institute for Water Security at the University of Saskatchewan (GIWS; HMB, JJH), Saskatchewan Water Security Agency (JJH: WSA-2012A-0001). The authors declare no conflict of interests.

Technical assistance: L. Aspden, K. Baranowska, D. Bayne, J. Bosch, E. Cavaliere, E. Cvetanovska, P. Dainard, P. Dubourg, R. Elgood, C. English, D. Evans, J. Findeis, B. Ginn, E. Hillis, V. Hiriart-Baer & Environment Canada Technical Operations, C. Hoggart, K. Hunter, B. Johnson, N. Kaur, G. Koehler, V. Kopf, K.E. Lindenschmidt, R. MacLean, S. McInnes, J. Miles, L. Molot, T. Ozersky, C. Quinn, Quinn's Marina, V. Sit, D. Vandergucht, L. Vasko, H. Wilson, D. Weber, S. Xu, H. Yip.

Supplemental Information

In addition to the $\delta^{18}O$-O_2 values used to model AR-^{18}O rates that we applied to estimate under-ice areal respiration (AR) rates on Blackstrap and Diefenbaker (Table 3), we also estimated under-ice respiration rates using continuous O_2 sensors and the free-water approach (Solomon et al. 2013).

On Blackstrap and Diefenbaker reservoirs we ice anchored (Block et al. 2019) continuous O_2 sensors in order to estimate under-ice pelagic community respiration rates. On Lake Diefenbaker at the Hitchcock Station (Fig. 1A) we deployed a Yellow Springs Instruments sonde (YSI, model 6600 V2) with a wiper on the continuous reading setting to collect temperature, turbidity, dissolved oxygen, specific conductance, and Chl a fluorescence in one hour increments. The sonde was deployed 81 days after ice-on (January 31, 2013) and recorded continuous data for 68 days until the batteries expired. The sonde was deployed at a depth ranging from 12.9–14.3 m due to the fluctuating water levels during this time period in this hydroelectric reservoir. Sonde O_2 concentrations were measured with a 6150 ROX Optical O_2 sensor (accuracy = ±0.1 mg L^{-1}, resolution = 0.01 mg L^{-1}), which underwent a 2-point calibration prior to deployment. On Blackstrap, we ice anchored 3 HOBO O_2 loggers (U26-001) which also employed optical O_2 sensors to measure O_2 concentrations (accuracy = ±0.2 mg L^{-1}, resolution = 0.02 mg L^{-1}), which also underwent a 2-point calibration prior to deployment. The sensors were deployed at depths of 3, 6, and 7 m from the ice surface at the Mountain station (Fig. 1A). The sensors were deployed 66 days after ice-on (December 14, 2012) and recorded O_2 in 15 minute increments until they had to be collected due to provincial ice safety regulations on March 19, 2013. Although no visible fouling was observed, the sensors were cleaned on a biweekly basis during their deployment. In order to estimate winter respiration rates, all data collected by the

continuous O_2 sensors and sonde was used for O_2 time series with a daily time step, which was then modelled using a linear regression model using the R package 'lm'. All data were tested for normality with the Shapiro Wilk test ($p < 0.05$) and were normally distributed. The O_2 time series from the 3 Blackstrap sensors were volume-weighted and then summed to get pelagic O_2 representative of that station. The O_2 concentrations (mmol m^{-3}) were regressed against time in order to estimate under-ice pelagic community respiration rates over the course of the winter (mmol m^{-3} day^{-1}; Suppl. Fig 1). We converted to areal rates by multiplying by the maximum depth of each station.

Areal respiration rates from the free-water approach were 9.0 and 70.0 mmol O_2 m^{-2} day^{-1} for Blackstrap and Diefenbaker, respectively. On Blackstrap, these rates are ~2x higher than those from the ^{18}O method, and 140x higher on Lake Diefenbaker (Table 3). The YSI O_2 sensors deployed on Lake Diefenbaker are twice as accurate as the HOBO sensors deployed on Blackstrap, which may help to explain the large differences in calculated rates. We believe the lack of agreement for under-ice AR rates on Lake Diefenbaker may be a result of the short deployment period (due to battery expiration), combined with the high flow rates that still occur under-ice (Pernica et al. 2017), resulting in complex mixing dynamics.

We assume that our sensor data represents the pelagic water column. There was no convective under-ice mixing at the Mountain station in Blackstrap, and in Lake Diefenbaker, the sonde was deployed below our estimated convective layer (Table 1, Pernica et al. 2017). The ^{18}O-derived AR rates on Lake Diefenbaker at the Hitchcock station from the depth closest to the sensors (7.5–18 m, n=3) are comparable (Table 3). We also assume that vertical diffusivity from sediments during the winter are low, and the O_2 measurements were not impacted by benthic respiration. In Canadian lakes, O_2 depletion rates within the sediment are 0.08 g O_2 m^2 d^{-1} in

oligotrophic lakes and 0.23 g O_2 m^2 d^{-1} in eutrophic lakes (Mathias and Barica 1980); rates for our mesotrophic reservoirs likely lie somewhere in between. Mathias and Barica (1980) also estimated O_2 decomposition within the water column to be ~0.01 g O_2 m^3 d^{-1}, rates significantly lower than what we are reporting here.

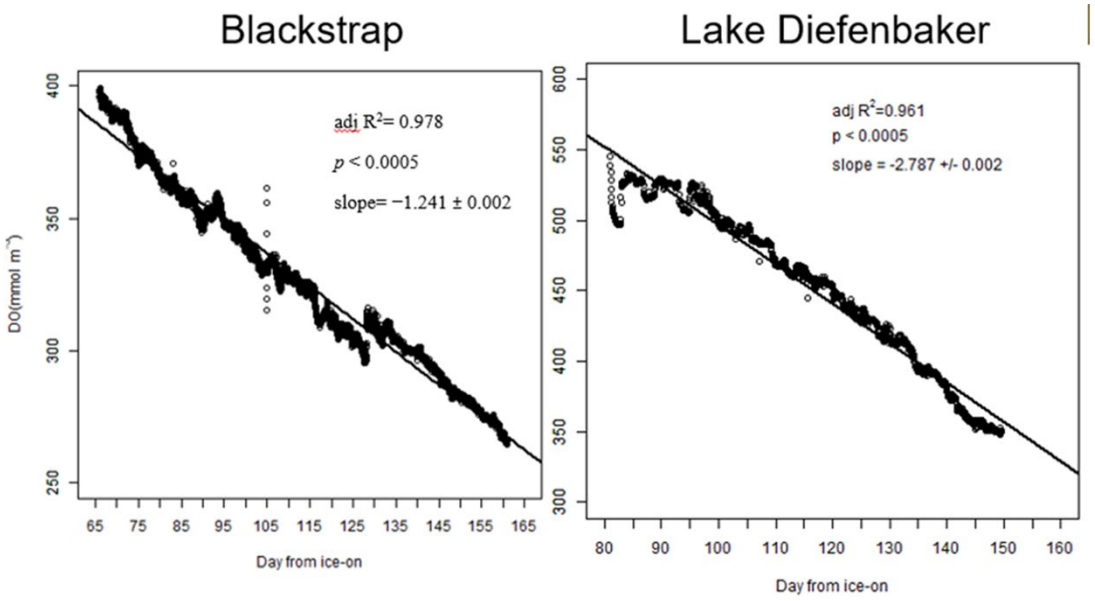

Suppl. Figure 1. Relationship between Dissolved Oxygen (DO) concentrations and days since ice-on from Blackstrap and Lake Diefenbaker, Saskatchewan, Canada. Continuous oxygen measurements were taken under-ice using sensors, and the slope of the O_2 decline over the course of the winter is indicated by the significant regressions.

References

Block, B. D., B. A. Denfeld, J. D. Stockwell, and others. 2019. The unique methodological challenges of winter limnology. Limnol. Oceanogr. Methods **17**: 42–57. doi:10.1002/lom3.10295

Mathias, J. A., and J. Barica. 1980. Factors Controlling Oxygen Depletion in Ice-Covered Lakes.

Can. J. Fish. Aquat. Sci. **37**: 185–194. doi:Doi 10.1139/F80-024

Pernica, P., R. L. North, and H. M. Baulch. 2017. In the cold light of day : the potential importance of under-ice convective mixed layers to primary producers. Inl. Waters **7**: 138–150. doi:10.1080/20442041.2017.1296627

Solomon, C. T., D. A. Bruesewitz, D. C. Richardson, and others. 2013. Ecosystem respiration: Drivers of daily variability and background respiration in lakes around the globe. Limnol. Oceanogr. **58**: 849–866. doi:10.4319/lo.2013.58.3.0849